THE UNIVERSITY OF ALBERTA

^{14}C-Misonidazole Biodistribution in BALB/C Mice Bearing EMT-6 Tumors

by

Bonnie Garrecht

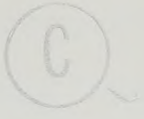

A THESIS

SUBMITTED TO THE FACULTY OF GRADUATE STUDIES AND RESEARCH IN PARTIAL FULFILMENT OF THE REQUIREMENTS FOR THE DEGREE OF MASTER OF SCIENCE

IN

EXPERIMENTAL RADIOLOGY

DEPARTMENT OF RADIOLOGY

EDMONTON, ALBERTA

FALL, 1982

DEDICATION

To my family, for their encouragement and support.

ABSTRACT

The biodistribution of ^{14}C-Misonidazole in tumor-bearing BALB/C mice shows that radiolabelled-species are uniformly distributed almost immediately after injection but that they leave all normal tissues, except the liver, to a greater extent than from the tumor. The clearance of the label has 2 phases: a rapid initial clearance, (43 minute half life), followed by slower 55 hour half life phase. Tumor to tissue ratios are enhanced by multiple dose administration. This enhancement could be related to the presence of hypoxic cells in tumors.

If the hypoxic cells in the tumor alone are considered, rather than the tumor as a whole, the amount of misonidazole bound to them would result in a tumor to tissue ratio of 30 to over 100 for single or multiple injections, respectively. Such ratios would be more than adequate for use of the drug as a clinical tool for investigating hypoxia within tumors.

Isoproterenol is used to induce myocardial infarcts in the hearts of mice. Associated with such infarcts is a zone of hypoxia or ischemia, and ^{14}C-Misonidazole appears to have an affinity for these hypoxic zones. There is a 2 fold increase in uptake of misonidazole in the hearts of isoproterenol treated mice compared with controls.

Whole body autoradiographs provide a visual demonstration of the biodistribution of ^{14}C-Misonidazole in BALB/C mice. They illustrate the heterogeneity of tumors and provide an independent confirmation of the biodistribution data obtained with liquid scintillation counting techniques.

ACKNOWLEDGEMENTS

Thanks to Dr. Cam Koch and Mr. Bert Meeker for their technical advice in the initial stages of the project.

I would like to thank the medical laboratory technologists at the Cross Cancer Institute for helpful discussions.

Special thanks are extended to Dr. Don Chapman whose enthusiasm for science made this most enjoyable. His encouragement and advice were invaluable.

Thanks to Bev Gartner for her excellent typing of the manuscript.

This research was supported in part by a grant from the Alberta Heritage Foundation for Medical Research.

TABLE OF CONTENTS

LIST OF TABLES

LIST OF FIGURES

LIST OF FIGURES

LIST OF PLATES

INTRODUCTION

Because of the variability of blood supply to a tumor, there are various degrees of oxygenation in its cells (1,2). Tumors can develop rather quickly and the blood supply may not be adequate to supply the needs of the entire tumor. Consequently necrotic regions result. Adjacent to these necrotic areas is a zone of cells distant from blood vessels, low in oxygen content and nutrients, but still viable. Adjacent to the capillaries within a tumor are the healthy proliferating tumor cells which have access to a good blood supply. When such a tumor is irradiated the oxygenated cells are most readily killed by the ionizing radiation. The necrotic core consists of dead cells and cell debris and does not have proliferative capacity so is of no concern. It is the hypoxic cells, resistant to the lethal effects of radiation, that limit eradication of the tumor. Once the oxygenated cells have been killed the hypoxic cells may become reoxygenated and resume growth. It is thought that hypoxic cells become reoxygenated during a fractionated course of clinical radiotherapy making the radiocure of some tumors possible.

That hypoxic cells are a factor in the curability of tumors by radiation has been the conclusion of several studies. By using high pressure oxygen during radio-

therapy, clinical investigators showed an enhanced cure rate, which they attributed to elevated oxygen tensions in the tumors (4,5,6,7). Another piece of clinical evidence is a study which showed that low hemoglobin levels correlated with high recurrence rates after radiotherapy in carcinoma of the cervix (8). Hemoglobin levels elevated by transfusions before radiotherapy to over 12g% to alleviate anemia, resulted in an improved radiocure rate (8) which could have been indicative of improved tumor oxygenation.

In addition to using oxygen as a sensitizer for the hypoxic cells in tumors, drugs which mimic the effect of oxygen can also be used. Chemical radiosensitizers have a potential advantage over oxygen because they are not consumed by respiring cells as they diffuse across the tumor (1). Thus a more uniform concentration of sensitizer across the tumor volume can potentially be achieved. Such drugs include metronidazole and misonidazole (MISO). Clinical studies using metronidazole, prior to radiotherapy, in patients with glioblastoma multiforme showed improved survivals over those patients not given the drug (9). Since this first study with metronidazole there have been numerous clinical trials and studies initiated for both metronidazole and MISO (10-22).

To demonstrate that hypoxic cells are a factor in the radiocurability of a tumor, tumors were made hypoxic artificially by blocking blood supply (26) or killing animals by asphyxiation (27) prior to irradiation. The different surviving fractions indicated the degree and importance of hypoxia in radiation resistance. Survival can be determined by observing tumor growth post irradiation (28) or by *in vitro* assays of surviving fractions (29). Further evidence of hypoxia in both human and animal tumor models has come from measurements of oxygen concentration within a tumor using oxygen electrodes (24,25).

Another means of examining the functional architecture of a tumor involves the injection of a radioactively labelled radiosensitizer such as MISO into a tumor bearing mouse (30). The drug is injected over a period of time to enhance the binding of MISO to the hypoxic tissues. After a 5 hour exposure to the drug, and 24 hours to allow for elimination of unbound MISO, the mouse was killed. The tumors were removed, washed in saline and fixed in formalin. Autoradiographs of these tumors clearly demonstrated that MISO does reach the tumor, and that it binds to what are most probably hypoxic cells. This assertion is based on the location of

the high uptake of radioactivity between the necrotic core and the peripheral oxygenated cells. These autoradiographs also demonstrate the heterogenous uptake of MISO in tumors as compared to the homogeneity found in a normal tissue such as liver. (See Plates A and B). Autoradiographs of ^{14}C-Misonidazole (^{14}C-MISO) labelled multicellular spheroids showed similar results. In vitro experiments have shown that MISO is preferentially bound to cells in a nitrogen atmosphere in higher amounts than that bound to similar cells in oxygen (23). (See Fig. 1). This suggested that MISO might be developed as a marker for hypoxic cells.

Tannock (31,32) has also demonstrated the presence of hypoxia in tumors by identifying proliferating cells which had incorporated ^{3}H-thymidine, and the necrotic core which had not. Intermediate to these two areas was a nonproliferating zone, low in oxygen content, which consistently had a lower labelling index.

Results from these and other experiments have strongly suggested that hypoxic cells are present in tumors, that their presence affects the eradication of the tumor by radiation and that hypoxic radiosensitizing drugs increase the radiosensitivity of animal tumors. Whether the amount of MISO that binds to hypoxic cells in tumors is significantly high relative to the amount bound

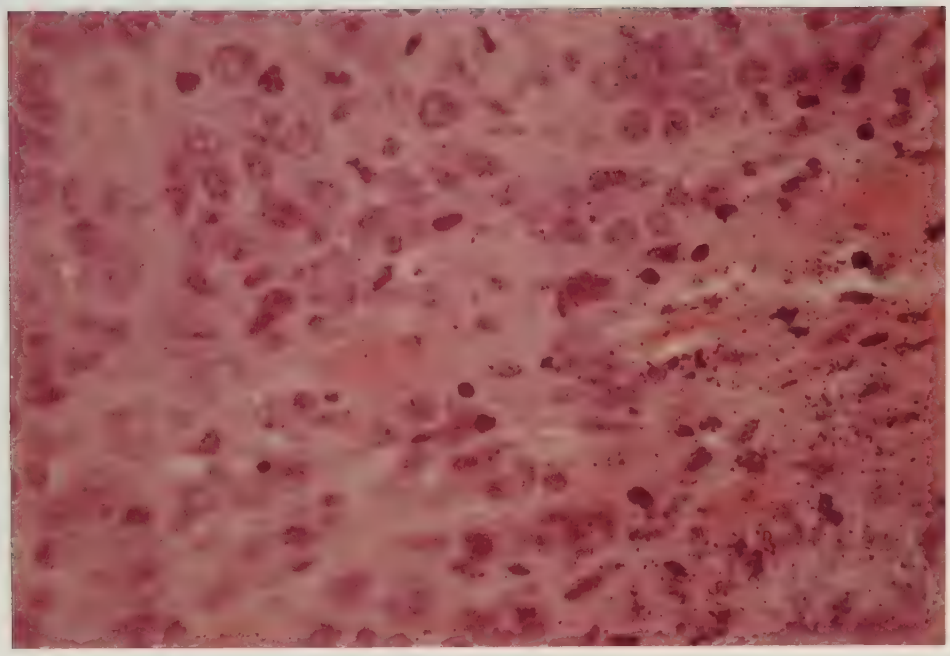

Plate A. Autoradiograph of EMT-6 tumor exposed to ^{14}C-MISO, demonstrating the heterogeneity of the tumor.

Plate B. Autoradiograph of mouse liver exposed to ^{14}C-MISO, demonstrating the homogeneity found in the liver.

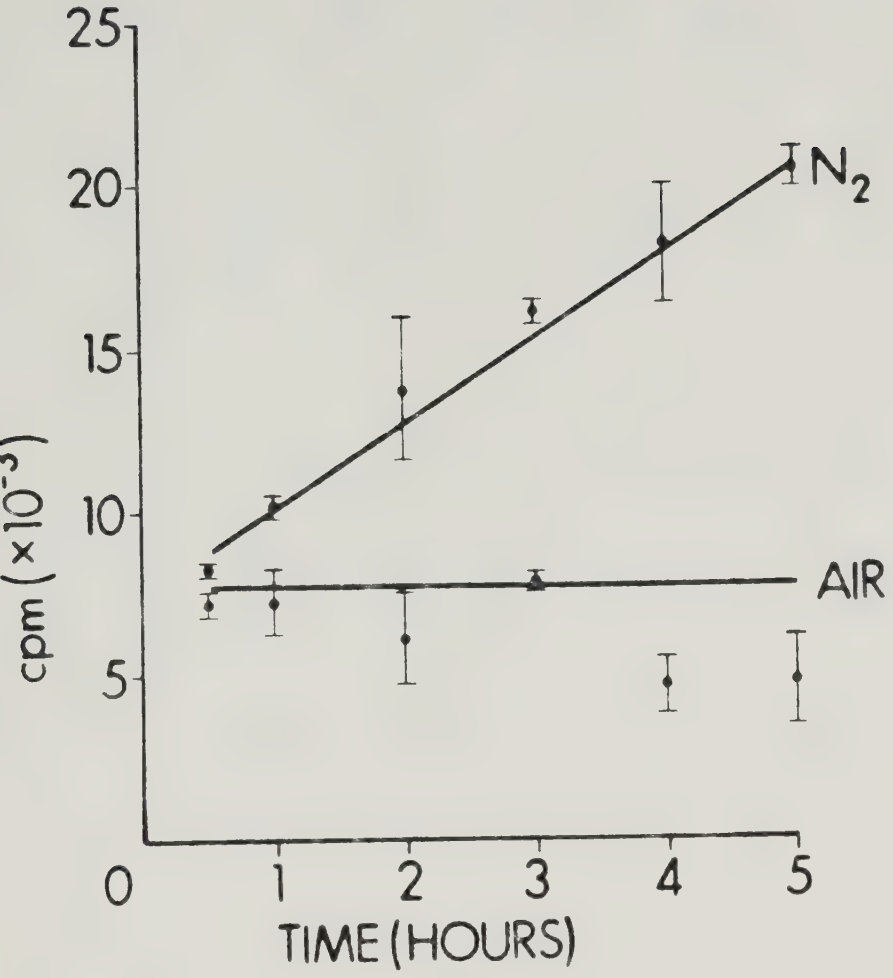

Figure 1. EMT-6 cells incubated with ^{14}C-MISO at 37°C in air, and in nitrogen ($\sim 5X10^5$ cells/sample). MISO is preferentially bound to cells in nitrogen.

in other tissues was not known. If it could be shown that the amount of drug bound to tumors was significantly higher than all normal tissues, this property might be exploited clinically for the detection of hypoxic cells in human tumors (1). If a gamma emitting radionuclide with appropriate half life and energy could be attached to the radiosensitizing drug, the distribution and extent of hypoxic zones within a tumor could be displayed by non-invasive methods using nuclear medicine techniques (1,30,33). This would be extremely valuable, not only because of the heterogeneity within the tumor itself (27) but also because of the variability among tumors (34). Once information was obtained about the tumor, the therapy regimen could be adjusted according to the degree of hypoxia within the tumor. If a significant portion of the tumor cells are hypoxic, radiation sensitizers, used to enhance cell death in the hypoxic zones, would improve the chances for a cure. An ideal gamma emitting label would have a half-life of about two to three days, and would not alter the behavior of the original drug. It also should be of high enough energy for detection, and not emit any particulate radiation which would contribute to the radiation dose without providing additional information. The half-life needs to be long enough to allow elimination of the unbound drug yet remain in the

tissue to provide a signal for the assay. Such a radiochemical might be bromine-77. It has a half-life of 57 hours and is produced by bombarding arsenic-75 with alpha particles (35). However, at present, there are no facilities in Alberta capable of producing bromine-77.

With the long term goal of developing a gamma-labelled marker for hypoxic cells in tumors in mind, the research described in this thesis with ^{14}C-MISO attempts to answer several questions. It deals with the techniques required for liquid scintillation counting and the construction of quench correction curves. It also examines the various types of quenching encountered in liquid scintillation counting. The whole body distribution, (particularly at long times), of ^{14}C-MISO in BALB/C mice bearing EMT-6 tumors is measured and it is also shown that ^{14}C-MISO can be selectively bound to hypoxic tissue aside from that found in tumors. The hearts of BALB/C mice were rendered ischemic by the administration of isoproterenol. ^{14}C-MISO is then injected and uptake monitored by liquid scintillation counting of the hearts and by autoradiographs. There is also a visual representation of the whole body distribution of the ^{14}C-MISO by whole body autoradiographs.

MATERIALS AND METHODS

Animals

All animal experiments were performed in the Radiobiology Animal Laboratory at the Cross Cancer Institute. Female BALB/C mice were obtained from the breeding stock of University Animal Services, Edmonton, housed at a maximum of 5 mice per cage, and fed rodent chow (Ralston Purina Co.) and water as desired. All mice weighed 20 to 25 g at time of experimentation.

Tumor Line and Induction

The tumor model selected was the EMT-6 tumor because it is known to have a significant hypoxic fraction of about 0.35 (36). The integrity of the cell line is maintained by alternate passage *in vivo* and *in vitro*. From two to four tumors are implanted subcutaneously in the flanks of BALB/C female mice by injection of approximately 2×10^6 EMT-6 cells in 0.05 ml Waymouth's medium (Gibco Laboratories). Tuberculin 1 ml syringes (Becton, Dickson & Co.) and 26 gauge 3/8" Yale needles (Becton, Dickson and Co.) were used. After 10 to 14 days the tumors were approximately 1 to 1.5 cm in diameter. Measurements are approximate because of the irregularity of tumor shape. Autoradiography of histological sections from some whole tumors was obtained. Tumors showing skin necrosis were not used in these experiments. The mice

were killed and the entire tumor was excised and weighed before being homogenized.

Liquid Scintillation Counting

When counting beta particle radioactivity the sample must be completely mixed with the liquid scintillation cocktail. This was achieved by first homogenizing the tissues using a Ten Broeck Tissue Grinder, pyrex^{R} brand, 15 ml capacity (Fisher Scientific Co.) (Nine parts of distilled water were added to the homogenized tissue to effect recovery of the sample.) The homogenate was mixed thoroughly before 100µl aliquots were dissolved in 1 ml of potassium hydroxide (Certified A.C.S. pellets, Fisher Scientific Co.). The KOH pellets had been dissolved in distilled water to make up a 1N solution. The samples, in glass scintillation vials, (Fisher Scientific Co.) were then put on an automatic shaker for one day, to facilitate dissolution. After the samples were completely dissolved, 1 ml 1N hydrochloric acid, (Certified 1N solution, 1.002-0.998 N, Fisher Scientific Co.), was added to each, to provide a neutral solution. To the neutral solution was added 15 ml Scintanalyzed^{TM} Scinti Verse (Fisher Scientific Co.). The vials were capped with polyseal^{R} liner caps (Fisher Scientific Co.) and shaken to thoroughly mix the contents, before being loaded into the Beckman LS7000 liquid scintillation counter. The

samples were counted with Program 4 which designated the channels as follows:

Channel A	lower limit 0	Channel B	lower limit 397
	upper limit 655		upper limit 655

The counter generated quench correction factors for each sample: $H^{\#}$ and sample channels ratio (SCR). Samples were each counted for 10 minutes. Background vials, vials containing everything but radioactive tissue, were counted with all samples.

Quench Correction Curves

The inherent variability in color and composition of the tissues compared in this study necessitated the construction of quench correction curves. Because efficiencies will vary among tissues, it is desirable to report the amount of radioactivity in disintegrations per minute (dpm). Counts per minute (cpm) detected by the counter will vary with the counting efficiency of each sample and so do not indicate the absolute amount of radioactivity present. Quench correction curves were generated in the following fashion. A homogenate of blood and liver was made by removing each from freshly killed BALB/C mice. The liver was minced up with scalpel blades. The blood and liver were then put in a 3 ml syringe (Becton, Dickson & Co.) and the mixture was pushed through successively smaller needles until a fine paste

resulted. Aliquots ranging from 0.01g to 0.12 g were measured into preweighed vials and then dissolved with 1 ml 1N KOH by agitating the capped vials on an automatic shaker. After sample digestion was complete, the samples were neutralized with 1 ml 1N HCl. A known amount of radioactivity was added to each vial by micropipetting ^{14}C-MISO into each of the vials. This was followed by the addition of 15 ml Scinti Verse. The vials were all shaken vigorously to thoroughly mix the contents, resulting in a clear solution of a color varying according to the amount of homogenate within.

The counting efficiency and corresponding quench correction factor for each sample was plotted on linear graph paper. The counting efficiency was calculated as follows:

$$\text{efficiency} = \frac{\text{cpm observed}}{\text{dpm added}}$$

To ensure the validity of the quench correction curves for the experiment, samples of all different tissues were taken and treated in the same way as the blood- liver homogenate. Results were plotted on the quench correction curve.

For the biodistribution study, dpm were determined with the following equation:

$$\text{dpm} = \frac{\text{cpm observed}}{\text{counting efficiency}}$$

Counting efficiency was determined by using the quench correction factors to correlate with an efficiency on the quench correction curve.

Drugs

Hoffmann LaRoche supplied the ^{14}C-MISO (1-(2-nitro-1-imidazole)-3-methoxy-2-propanol) labelled in the 2-position of the imidazole ring. The specific activity was 145μCi/mg. A 10mM stock solution of the drug was used for all the experiments.

DL-isoproterenol HCl (1[3",4'-dihydroxyphenyl] 2-isopropylaminoethanol HCl) (Sigma Chemical Company) was dissolved in saline immediately before use.

Injections of Drugs

All drugs were injected with 1 ml Tuberculin syringes and 25 gauge 5/8" needles (Becton, Dickson & Co.) intraperitoneally.

For single dose MISO work: 20μg ^{14}C-MISO/g mouse

For multiple dose MISO work:

time 0	20μg ^{14}C-MISO/g mouse
time 45 min	10μg ^{14}C-MISO/g mouse
time 90 min	10μg ^{14}C-MISO/g mouse
time 135 min	10μg ^{14}C-MISO/g mouse

For induction of myocardial infarcts with isoproterenol

day 1 75 μg/g or 200 μg/g mouse

day 2 Time 0 75 μg/g or 200 μg/g mouse

Time 3 hrs 20 μg/g mouse (^{14}C-MISO)

Time 4 hrs 10 μg/g mouse (^{14}C-MISO)

Time 5 hrs 10 μg/g mouse (^{14}C-MISO)

Biodistribution Study

After a selected time period (30 minutes to 72 hours), following single or multiple doses of ^{14}C-MISO, the mice were killed by cervical dislocation. Samples of normal tissue were removed from blood, heart, lung, liver, spleen, kidney, stomach, intestine, colon, bladder, ovary and uterus, fat, muscle and brain. When possible, entire organs were removed to avoid regional variations in uptake within organs. The exceptions to this were the colon, intestine, muscle and fat. Gut contents were removed before homogenation. Tissues were removed to preweighed vials and one in ten dilutions with distilled water were made of the homogenized tissues. Multiple 100μl aliquots of each sample homogenate were taken and dissolved in 1 ml 1N KOH. Samples were closed tightly with polyethylene lined vial caps and put on the automatic shaker to facilitate dissolution. Once dissolved, 1 ml 1N HCl was added followed by the addition of 15 ml Fisher Scinti Verse. The vials were shaken vigorously to ensure complete mixture of the contents.

Homogenates of tumors were made as with normal tissue, and were treated identically to the normal tissues.

Vials were loaded into the Beckman LS 7000 Liquid Scintillation Counter. Background vials were counted with the samples and environmental background counts were subtracted from each of the raw counts before any calculations were done. Once counts per minute and quench correction factors were obtained, efficiencies were determined from the quench correction curves and actual distintegrations per minute per sample were calculated.

The amount of activity in the tumor compared to the amount within normal tissue was expressed as a tumor to tissue ratio. It was calculated as follows:

$$\text{tumor to tissue} = \frac{\text{dpm in 100}\mu\text{l tumor homogenate}}{\text{dpm in 100}\mu\text{l normal tissue homogenate}}$$

Autoradiographs of Hearts

Experiments using autoradiographs required that the tissue be put in 10% buffered formalin after removal from the mouse. The formalin was changed every day for 5 days. The tissue was then embedded in paraffin wax and sectioned. Sections mounted on the microscope slides were dewaxed and then dipped in liquid emulsion (Kodak NTB3), using a darkroom. Slides were placed in lightproof containers for 3 weeks and after development of the emulsion, the sections were stained with the

hematoxylin-basic fuchsin-picric acid (HBFP) stain (37). This stain demonstrates myocardial ischemia.

Autoradiographs of Tumors

For the autoradiographs of tumors, mice were injected according to the following regimen:

Time 0 20 μg ^{14}C-MISO/g mouse

Time 1 hour 10 μg ^{14}C-MISO/g mouse

Time 2 hrs 10 μg ^{14}C-MISO/g mouse

Time 3 hrs 10 μg ^{14}C-MISO/g mouse

Time 4 hrs 10 μg ^{14}C-MISO/g mouse

The mouse was killed 24 hours after time 0. The tumor tissue was removed and washed in saline. The tissue was treated exactly the same way as the heart tissue, except after development of the emulsion the slides were stained with hematoxylin and eosin stain.

Whole Body Autoradiographs (ARG's)

This procedure involved freezing of the mouse in liquid nitrogen immediately after death. The frozen mouse was then embedded in a block of methyl cellulose (Fisher Scientific Co.) and left to freeze solid for 30 minutes. The microtome and blades were all kept in a freezer for the entire process of sectioning. The block containing the mouse was put on the microtome and 20μm sections were taken. In order to remove the section from the block, Scotch 3M tape was used to lift the section as it was cut. The sections were put in a box containing silica

drying beads and returned to the freezer. They were left to dry for several days and then the sections were put on mammographic film. The sections and film were kept in the freezer until the appropriate exposure time had elapsed. The films were then developed. Whole body ARG's procedures were performed at Brookhaven National Laboratory in collaboration with Dr. Brill and Dr. Som.

CHAPTER ONE

LIQUID SCINTILLATION COUNTING

INTRODUCTION

Because carbon-14 is a beta emitting radionuclide, liquid scintillation counting techniques are required for the measurement of drug uptake using the drug thus labelled. This entails a certain amount of sample preparation, but can be as reliable and reproducible as any direct measurements of other forms of radioactivity such as gamma emissions. Of the beta emitters, using the carbon-labelled compound is preferable to using the tritiated compound because of carbon's higher energy (0.159 MeV Emax for C-14 compared to 0.018 MeV Emax for H-3) (35), making it less subject to attenuation by quenching. Quenching is interference with counting efficiency (38). In liquid scintillation counting, 'counts' are generated by the beta particles excitation of solvent molecules. The beta particles are immersed in an aromatic solvent which has pi electrons easily excited by the radiation. The excitation of the solvent molecules is then transferred to solute or scintillant molecules. Light photons are emitted by the solute upon deexcitation. After amplification, the photons are detected by coincident photomultiplier tubes (39). Anything that interferes with the production of light photons by the

solvent or the detection of the photons by the photomultiplier tubes is said to quench or reduce counting efficiency.

There are various types of quenching. Chemical quenching interferes with the transfer of the beta particle's energy to the solvent by accepting the excitation of the radiation without the emission of light (40). Chemicals that are more easily excited than the solvent molecules are aliphatic ketones, amines and halogenated compounds (41). Dilution quenching also interferes with the production of photons (40). But rather than chemically interfering with the energy transfer, it merely prevents the excited molecules from ionizing the excitable molecules by separating them physically. Aliphatic ethers, esters and alcohols are diluters (41).

Color quenching will reduce counting efficiency because it interferes with the optical detection of the light photon by the photomultiplier tubes (40). There is efficient production of light but it is absorbed by colors in the solution. Red colors are the most effective absorbers of the emissions whereas blue colors are the least effective (42). This form of quenching occurs because the emissions match the absorption spectrum of

the color. Obviously, a clear colorless solution is desirable to avoid color quenching.

Quenching can be due to other physical factors as well (42). If the radioactive material is insufficiently digested to be in intimate contact with the solvent molecules, some beta emissions will be absorbed by the tissue rather than ionize solvent molecules. Complete digestion of the sample and its uniform and intimate mixing with the scintillation solvent or fluor are vital for accurate counts to be obtained. Surface absorption of radioactive molecules onto the vial wall reduces counting efficiency by up to one half. The counting geometry is changed from that of a sphere (4 pi geometry) completely immersed and surrounded by solvent, to one half of a sphere (2 pi) exposed to the liquid scintillation cocktail. Quenching also results when the sample precipitates out of solution. Phase formation will also decrease counting efficiency because the radioactive molecules will be unevenly distributed between the aqueous and nonaqueous phase. Only the radioactive molecules in contact with the scintillation cocktail will be detected. Many of these problems can be alleviated by proper sample preparation. Some factors, such as sample precipitation and phase separation can be easily detected when using glass scintillation vials.

Glass scintillation vials have several advantages over the rather opaque polyethylene vials. Although glass vials are expensive and their disposal presents a problem, irregularities within the vial can be seen. Offending samples can then be eliminated from the experiment. Glass vials are impermeable to solvents whereas polyethylene vials may allow fluor to seep out (43). This would result in a gradual loss of counts as well as contamination of the liquid scintillation counter. The counting efficiency in plastic vials may be a few per cent lower than with glass vials due to absorption of light (42). This is a more critical problem when dealing with low energy emissions. Polyethylene lined vial caps were used rather than foil lined ones because foil is attacked by the basic reagents used to dissolve tissue (44). This contaminates the sample resulting in severe quenching.

Even though precautions are taken to prevent excessive sample variability, the inherent variability in color and composition of the tissues used in a biodistribution study necessitates the use of quench correction methods. Using quench correction curves was preferable to the internal standard quench correction method because it has been shown to be much more dependable and accurate (45). The internal standard method involves adding a

known amount of radioactivity to each sample vial to determine the counting efficiency of each sample (46). The standard must be added to the same phase that the radioactivity is in, and it must be added to each vial. Each vial must then be counted a second time. This becomes very time consuming. The sample cannot be recounted or recovered once standard has been added. Opening the vial to add the standard may add contaminants which act as quenchers. Water can be a strong quencher, and opening a refrigerated vial to add the standard could lead to condensation of moisture in the vial. This method could also be expensive, especially when dealing with large numbers of samples and samples with high activity.

Quench correction curves are thus preferable to the internal standard method of quench correction. Using quench correction factors and curves to determine counting efficiency involves the use of many observations at varying sample concentrations to simulate the variety encountered in an experiment (45). Plotting a quench correction curve simplifies the assay of the experimental samples because samples only need to be counted once, and they are not disturbed once they have been prepared. In this thesis, the quench correction factors generated by the Beckman LS700 Liquid Scintillation Counter were the $H^{\#}$ and sample channels ratio (SCR). The $H^{\#}$ is a measure of

the shift of the leading Compton edge of the unquenched external standard spectrum to the quenched external standard spectrum (39). The standard is an external standard of $^{137}Cs/\ ^{133}Ba$. This is an indicator of the shift in the sample spectrum. The sample channels ratio is a measure of the change from the unquenched to the quenched sample spectrum (47). Rather than an absolute value like the $H^{\#}$, it is a ratio. In the Beckman liquid scintillation counter,

$$SCR = \frac{\text{counts in channel B}}{\text{counts in channel A}}$$

Therefore as quenching increases the SCR value will decrease. A drawback to the SCR quench correction method is seen with low activity samples which require often unreasonable lengths of time to accumulate adequate counts for the ratio calculation. Occasionally it is not possible to get a statistically valid SCR because of low counts.

An advantage of the use of SCR quench correction curves is that the type of quenching agent has little or no effect on the type of quenching that occurs (40,48). Hence, one curve can be used to correct for the presence of different quenchers and no distinction need be made between color and chemical quenching. Once the curves are generated they are available for use in all the experiments described here and allow for conversion of the cpm generated by the counter to dpm required for comparisons.

RESULTS

After the preparation of the quench standards, quench correction curves were generated. The counting efficiency and corresponding quench correction factor for each sample was plotted on linear graph paper. The efficiencies ranged from about 50% for the dark yellow solutions with high amounts of blood-liver homogenate to about 75% for the colorless solutions. (See Fig. 2 and 3).

To ensure the validity of the quench correction curves for the experiments of this thesis, samples of all the different tissues were taken and treated in the same way as the blood-liver homogenate. Efficiencies were calculated and plotted on the quench correction curve. There was good correlation between the blood-liver homogenate and various tissues, indicating that the curves were suitable for use in this experiment.

DISCUSSION

Good correlation was obtained between the experimental samples and the quenched standards used for the construction of the quench correction curves. These quench correction curves were used in the calculation of efficiencies throughout the experiments of this thesis. Efficiencies of 50 to 75% are lower than the ideal value of 90% efficiency for C-14 (39). However all values were converted to dpm, so the lower efficiencies would be accounted for.

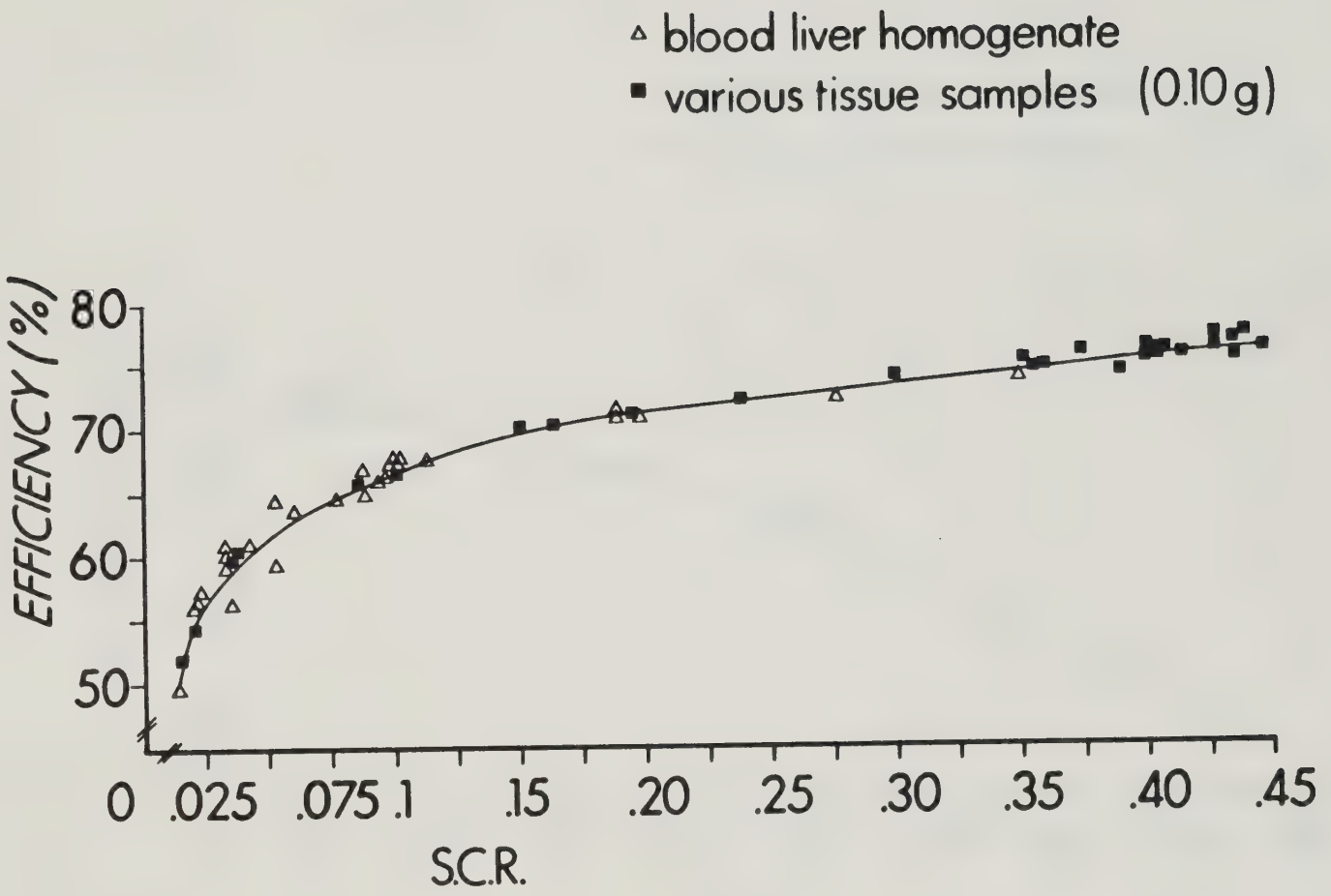

Fig. 2. Quench correction curve (efficiency vs. S.C.R.)

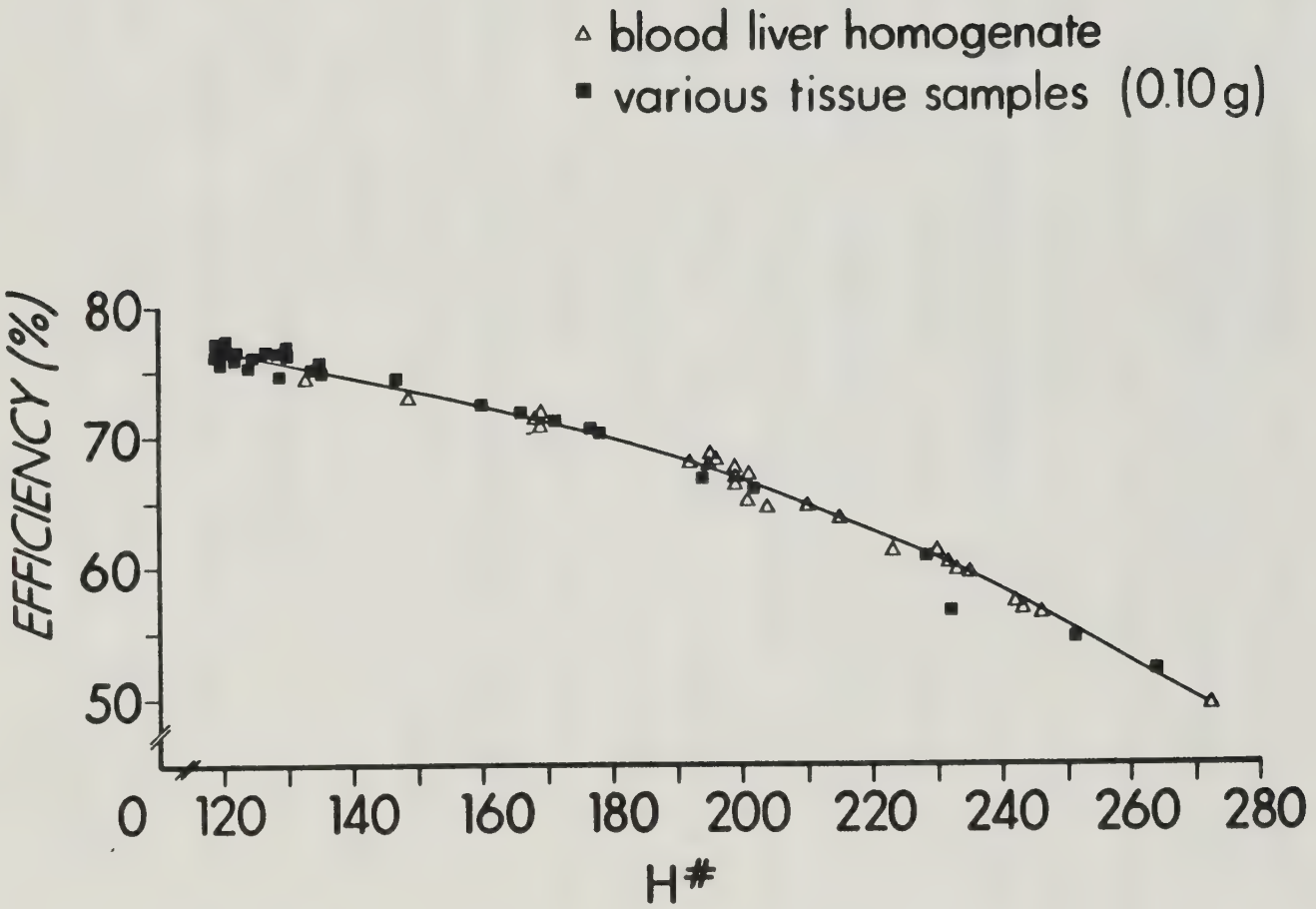

Fig. 3. Quench correction curve (efficiency vs. $H^{\#}$)

CHAPTER TWO

DISTRIBUTION OF ^{14}C-MISONIDAZOLE IN BALB/C MICE BEARING EMT-6 TUMORS

INTRODUCTION

The pharmacokinetics and metabolism of any drug play major roles in its biodistribution. Because they were not specifically studied in the experiments of this thesis it is valuable to review previous studies of the metabolism and pharmacokinetics of MISO and other sensitizers.

There are several ways of analyzing a drug's behavior. Assay techniques for nitroimidazoles include high performance liquid chromatography (HPLC), gas-liquid chromatography (GLC), thin-layer chromatography (TLC), polarography, colorimetry, uv spectrophotometry and radioactive tracer study (50). The specificity of these assay methods range from separation and quantitation of metabolites to a measurement of total drug present. When using a radiolabelled drug there is a determination of the behavior and distribution of all radiolabelled species, whether they are the active moeities or not. So in doing this biodistribution study with ^{14}C-MISO references to biodistribution of ^{14}C-MISO actually refer to the ^{14}C-label.

There are various routes of radiosensitizer administration. Intravenous administration results in instan-

taneous distribution of the drug within the central compartment of the body (50). This includes highly perfused tissues and the blood. The drug is then metabolized and excreted, and enters the peripheral compartment (skin and muscle). After an oral or intraperitoneal dose of sensitizers, there will be a delay in distribution because there must be absorption from the site of administration. However once the drug is absorbed the half lives are the same for both intravenous and intraperitoneal injection (49,50). Workman (50) reports a half life for MISO of 0.33 to 0.66 hour in mice.

Different half lives for radiosensitizing drugs have been reported by other workers. Chin and Rauth (49) report a half life for MISO of 1 to 1.5 hours after intravenous or intraperitoneal administration in mice. After a dose of 0.5 mg/g body weight, they found the radioactively labelled MISO to be widely and rapidly distributed to all tissues. Following oral or intraperitoneal administration of drug, radioactivity levels were highest in the liver, followed by the kidney, spleen, heart, lung, testes, brain, muscle and skin. They also found some accumulation of radioactivity in the gut. Chromatographic analysis of liver fractions showed

complete metabolism of MISO in that organ (49). MISO was largely eliminated via urinary excretion as well as excretion with the feces. A large portion of the activity eliminated from the gut may have arisen from radioactive bile being excreted from the liver into the lumen of the gut.

The metabolism of MISO results in several products (49,65). Metabolites are similar whether the drug is given to humans or mice. They include unchanged MISO, desmethyl-MISO, an aminoimidazole and glucoronides of MISO. The C-14 label is in the 2-position of the imidazole ring of MISO and all measurements of MISO and its derivatives are associated with this label.

RESULTS

Following a single dose (20μg/g body weight) of ^{14}C-MISO, there appeared to be three phases of distribution of the radiolabelled fragments. The first phase was the distribution to all body components from the intraperitoneal site of injection. This was very rapid and essentially complete within 30 minutes. Figures 4-18 show that there was no further uptake in any of the tissues examined after 30 minutes post injection. The second phase could be called the elimination or excretion phase. There was a fairly rapid (43 min half life) elimination of ^{14}C-MISO and ^{14}C-desmethyl MISO from all tissues

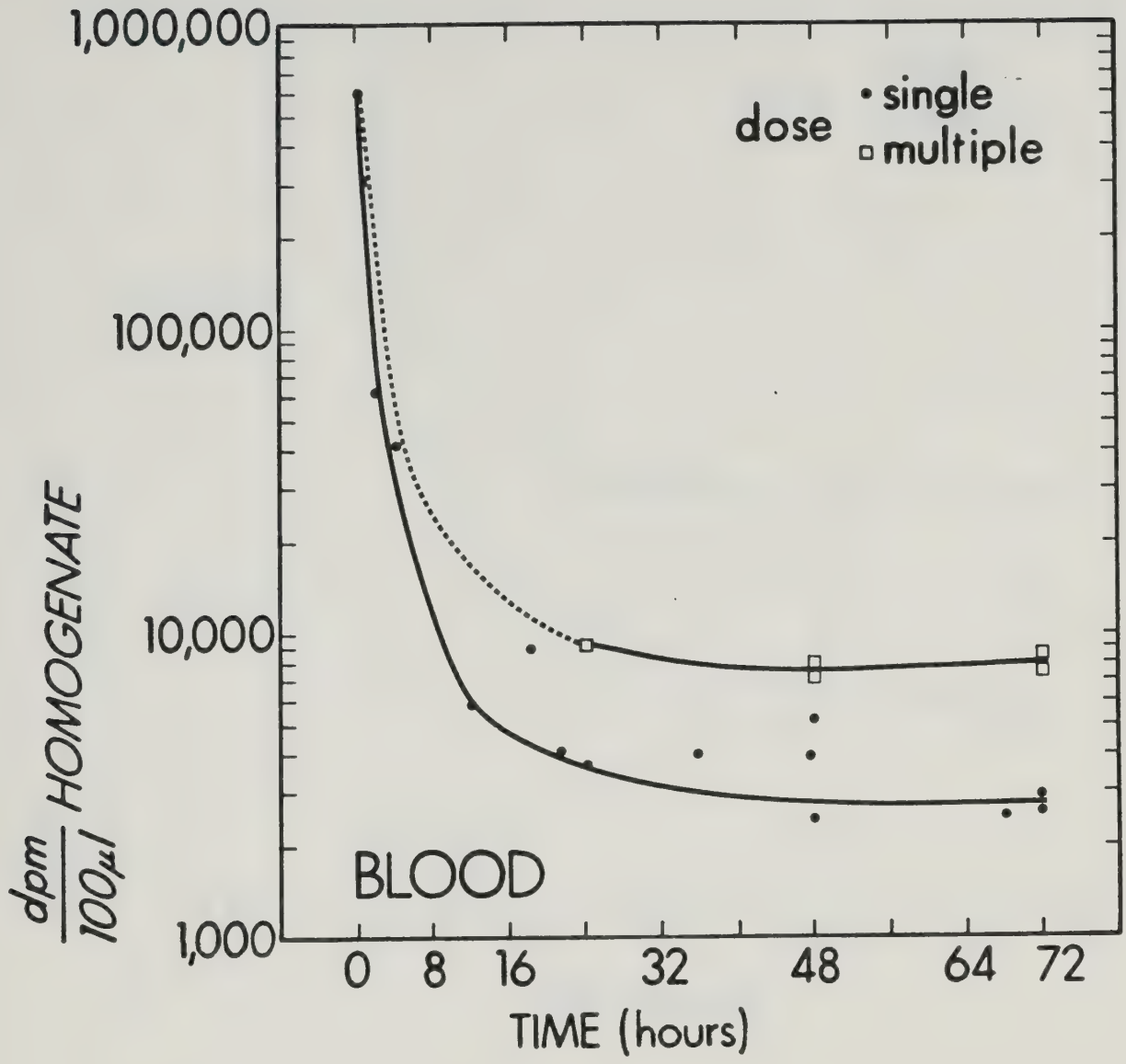

Fig. 4. Amount of ^{14}C-MISO in mouse blood

correlation coefficient -0.70 Slope -83.28 for final elimination phase (post 18 hrs.)

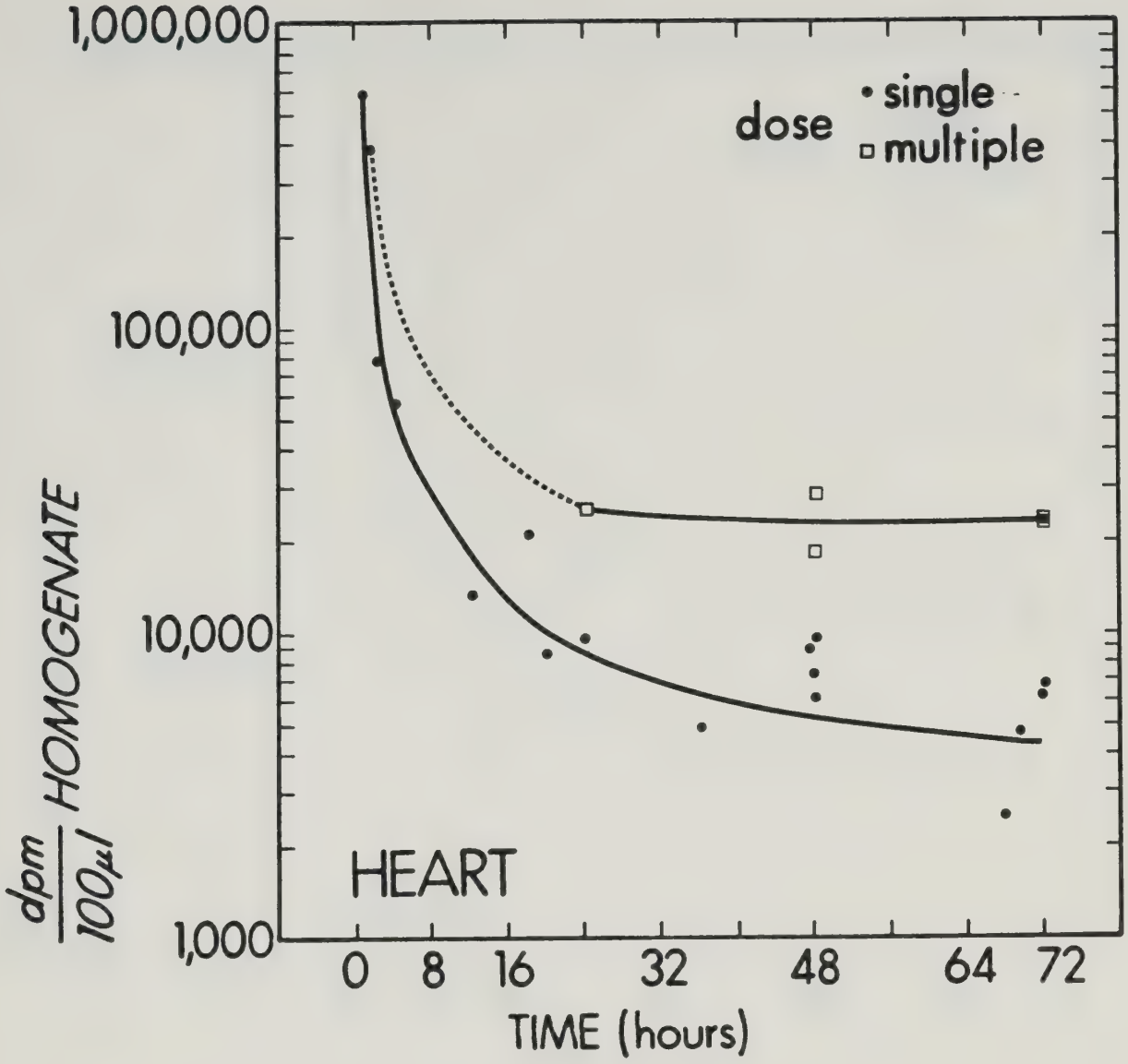

Fig. 5. Amount of ^{14}C-MISO in mouse heart

correlation coefficient: -0.57 Slope -67.08 for final elimination phase (post 18 hrs).

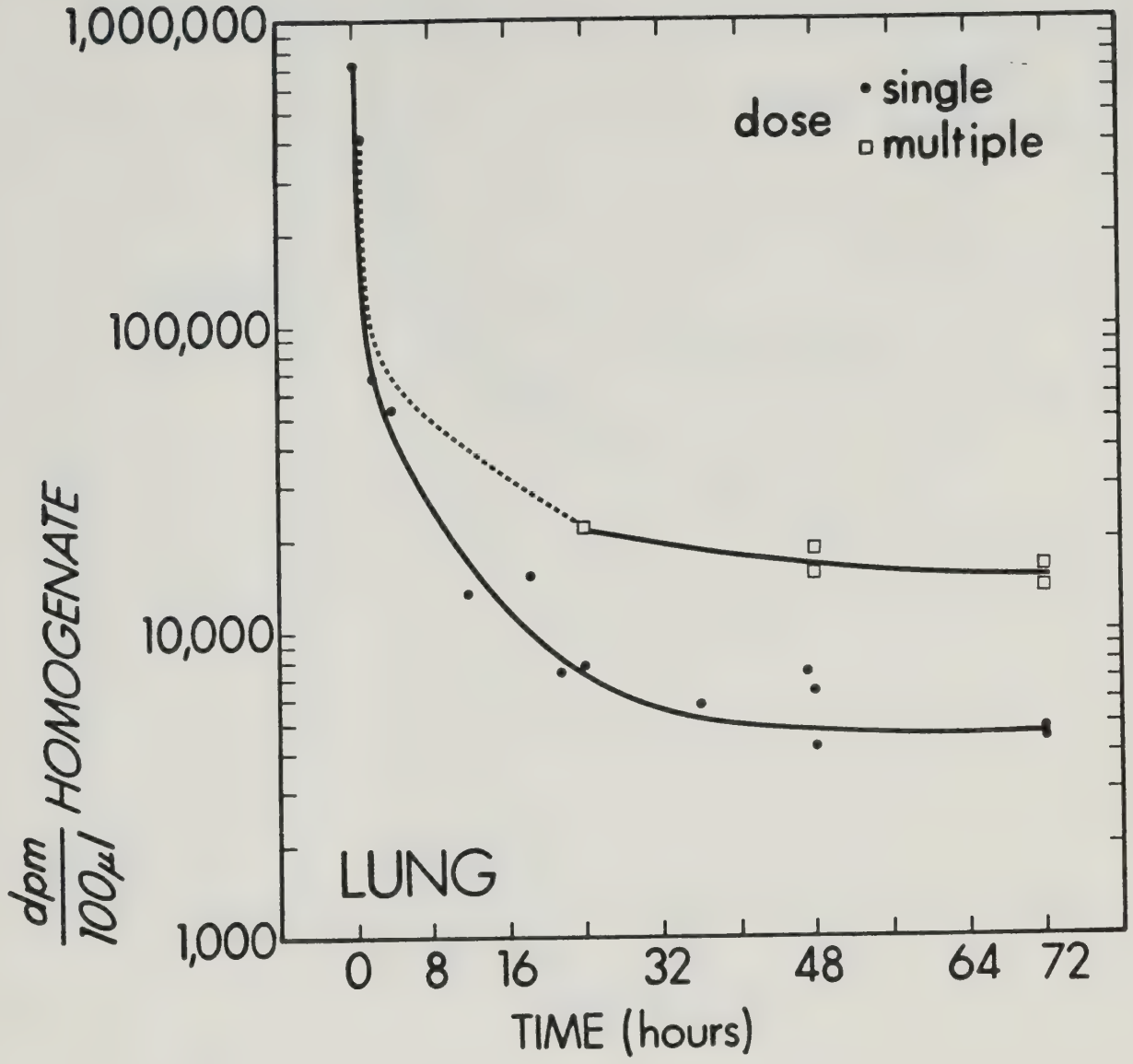

Fig. 6. Amount of ^{14}C-MISO in mouse lung

correlation coefficient: -0.78 Slope -96.55 for final elimination phase (post 18 hrs).

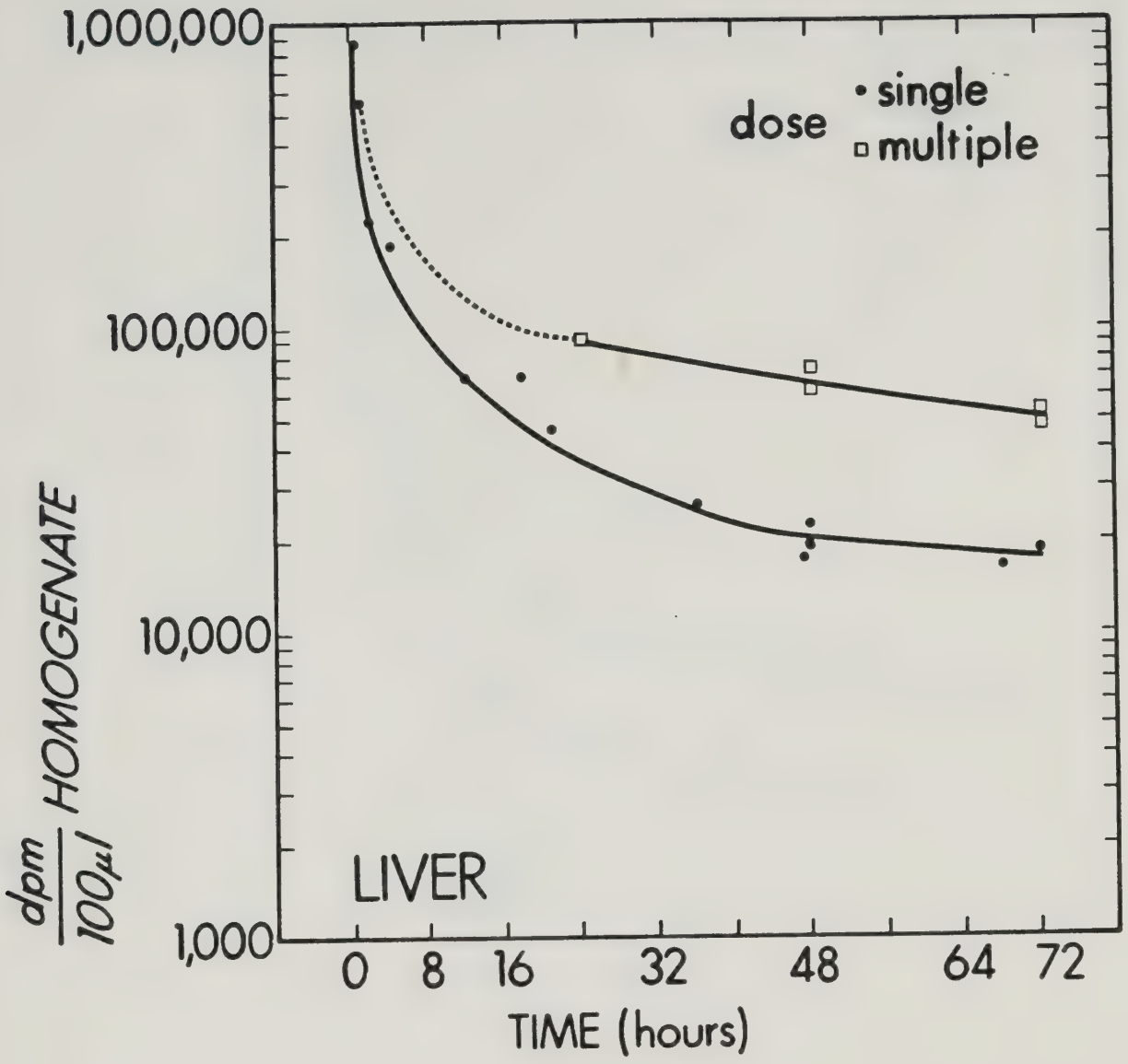

Fig. 7. Amount of ^{14}C-MISO in mouse liver

correlation coefficient: -0.87 Slope -79.18 for final elimination phase (post 18 hrs.)

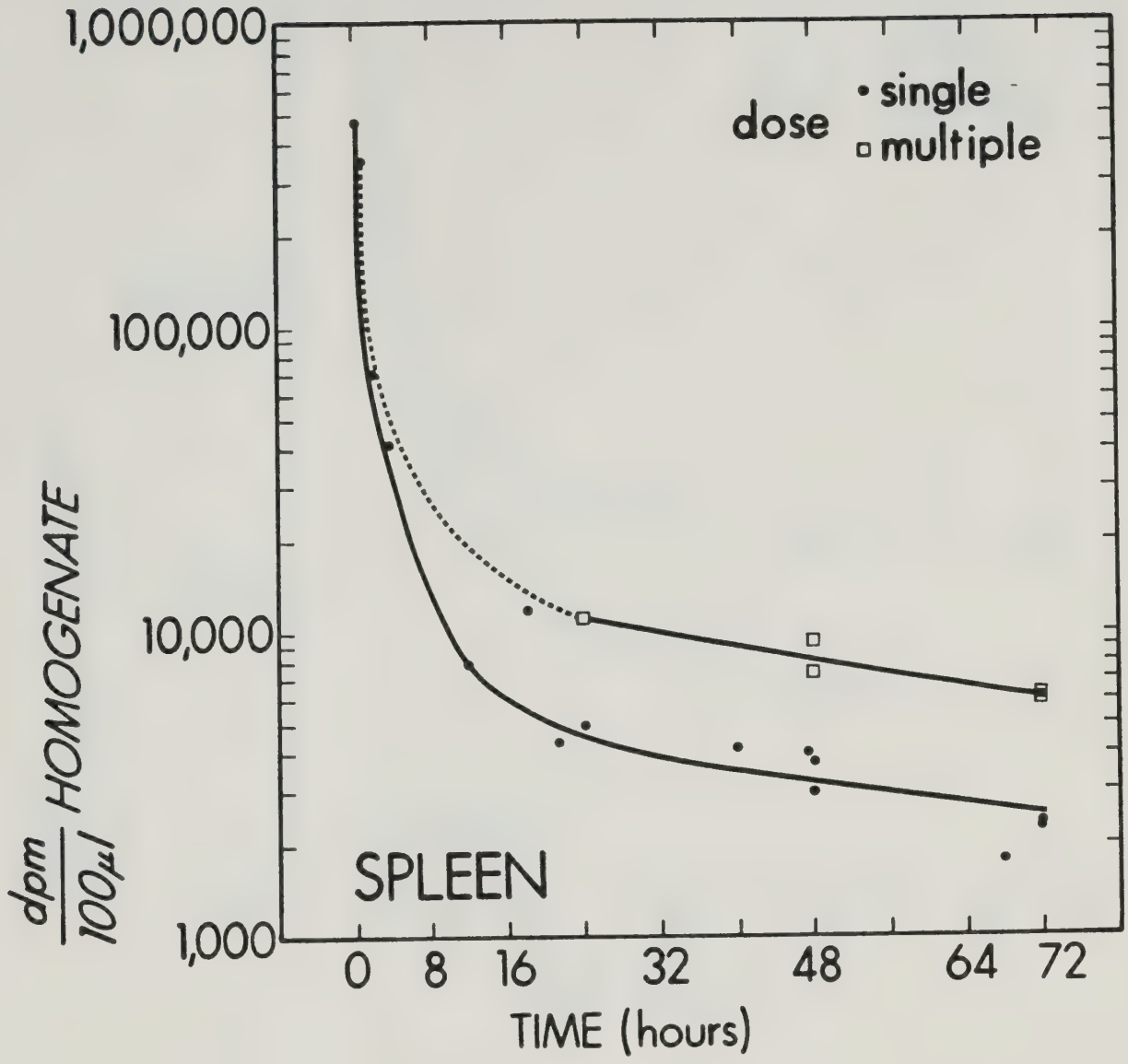

Fig. 8. Amount of ^{14}C-MISO in mouse spleen

correlation coefficient: -0.87 Slope -77.81 for final elimination phase (post 18 hrs.)

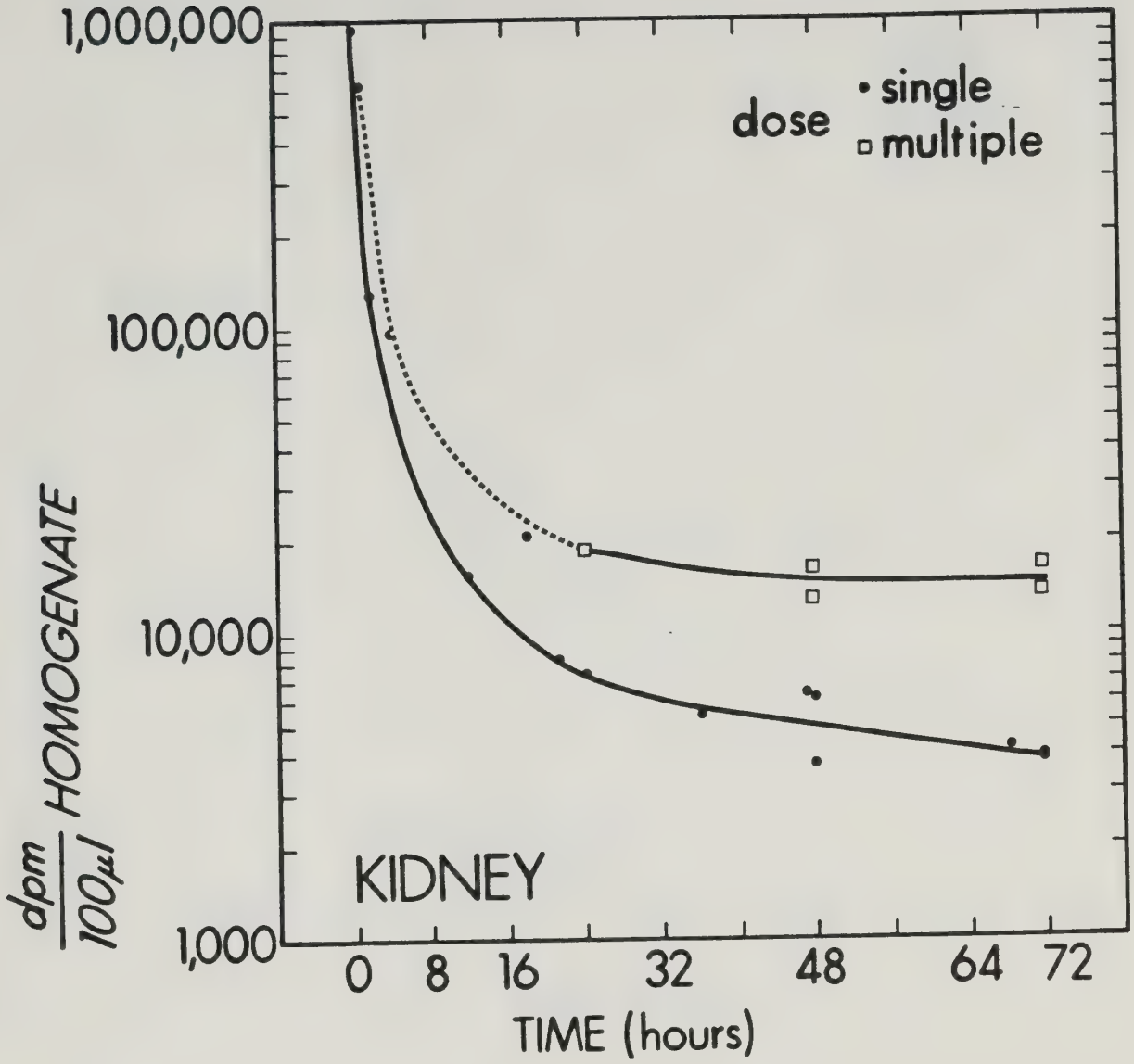

Fig. 9. Amount of ^{14}C-MISO in mouse kidney

correlation coefficient: -0.81 Slope -72.96 for final elimination phase (post 18 hrs.)

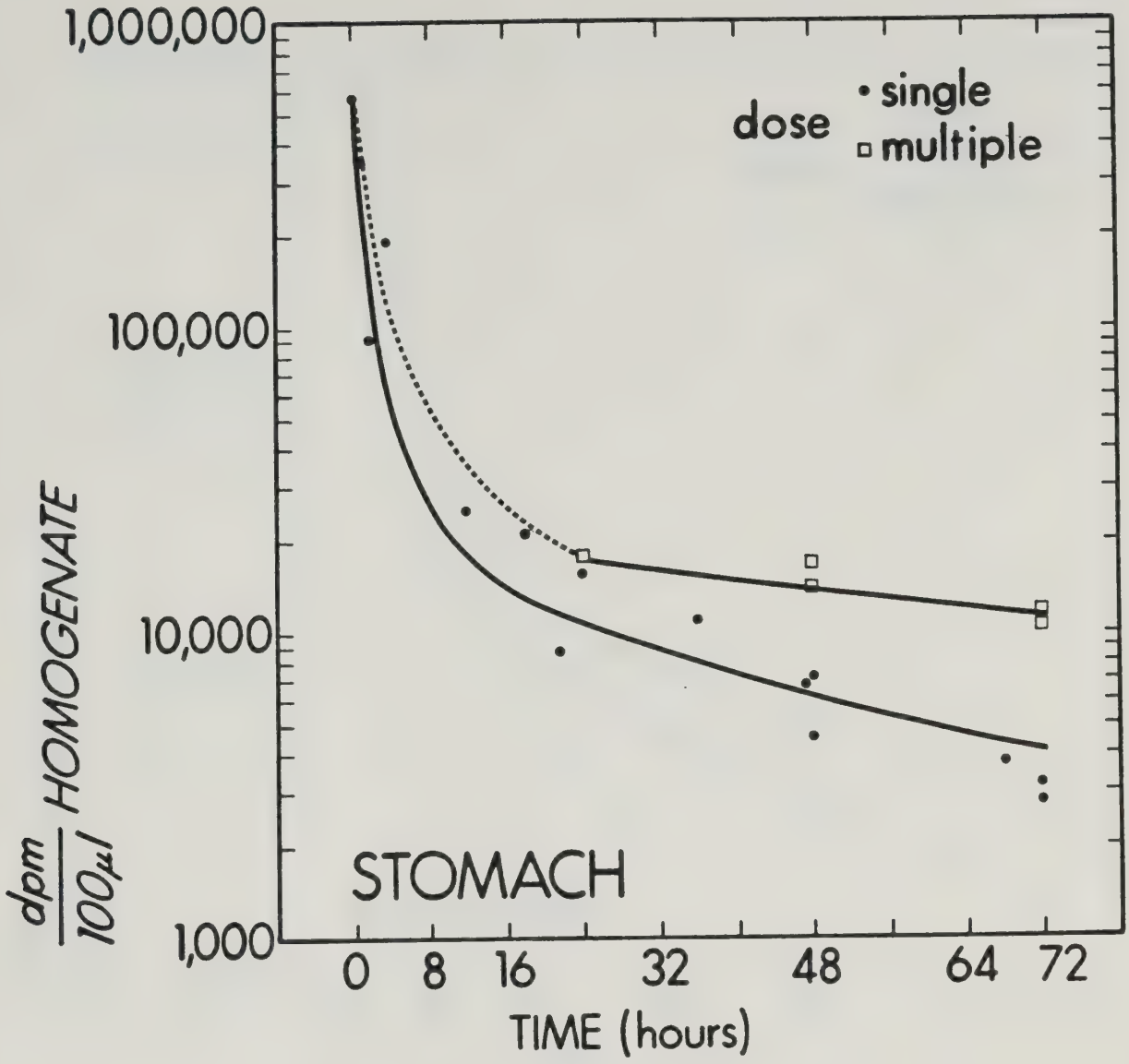

Fig. 10. Amount of ^{14}C-MISO in mouse stomach

correlation coefficient: -0.93 Slope -63.98 for final elimination phase (post 18 hrs.)

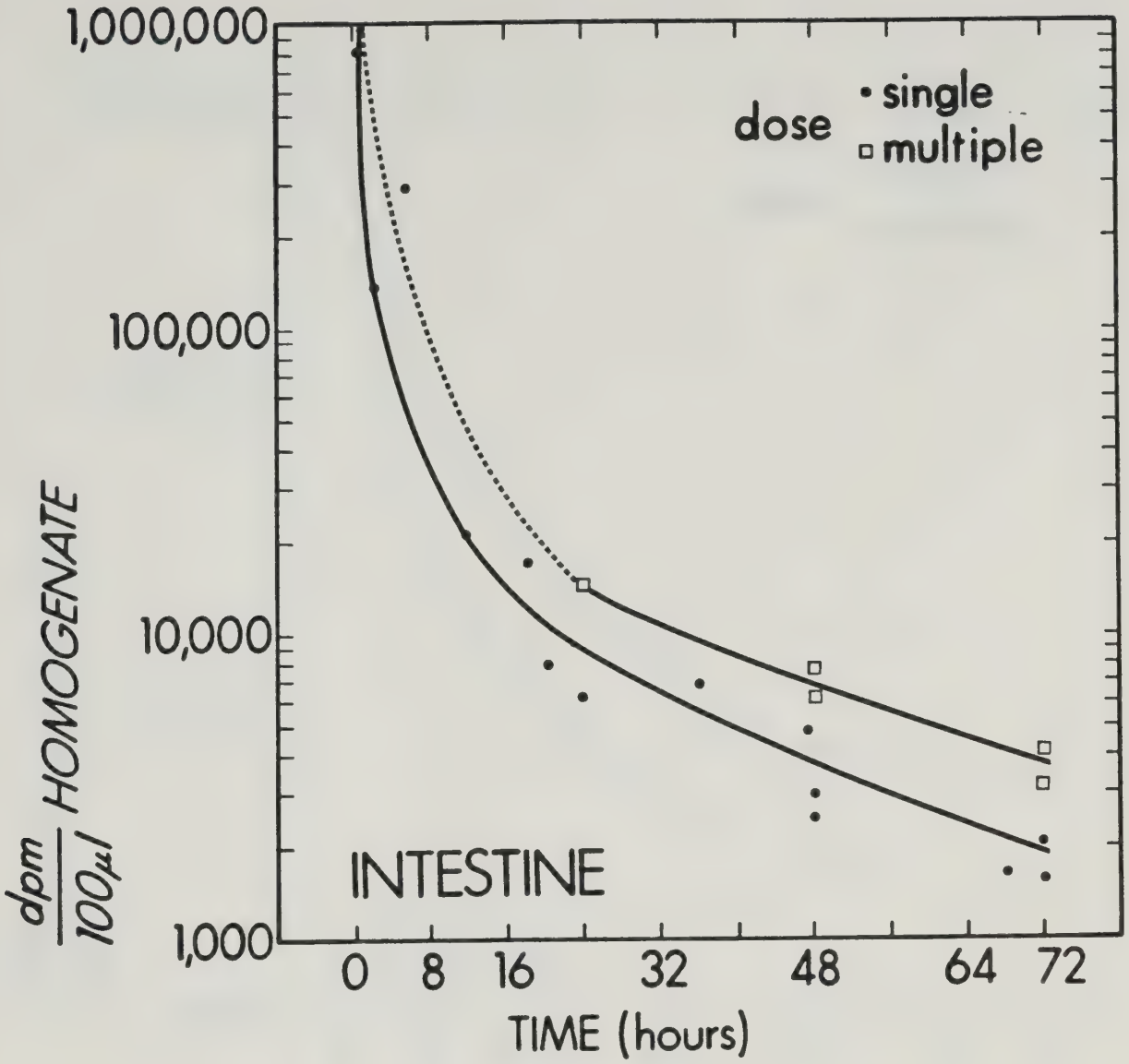

Fig. 11. Amount of ^{14}C-MISO in mouse intestine

correlation coefficient: -0.93 Slope -56.31 for final elimination phase (post 18 hrs.)

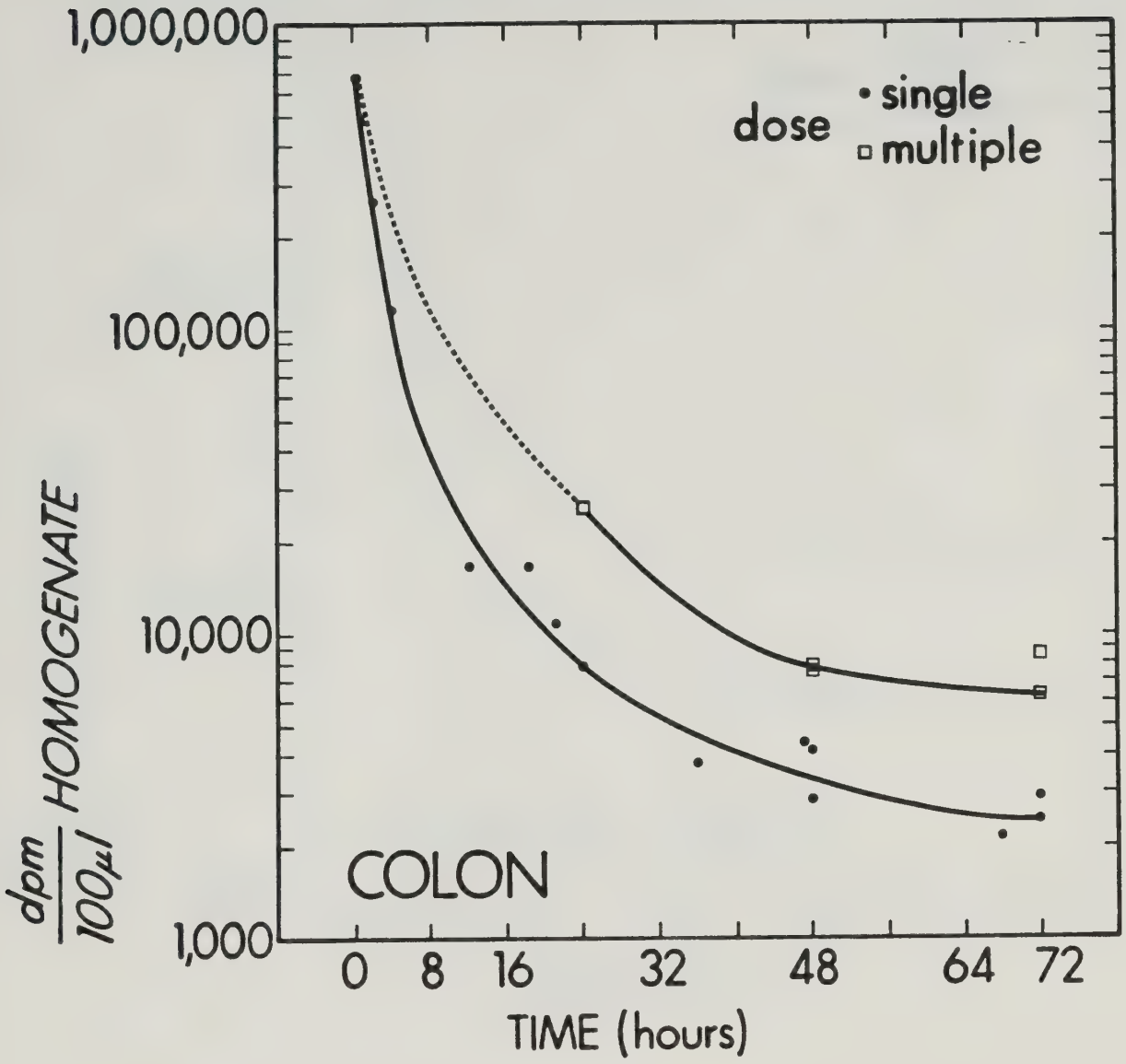

Fig. 12. Amount of ^{14}C-MISO in mouse colon

correlation coefficient: -0.90 Slope -63.23 for final elimination phase (post 18 hrs.)

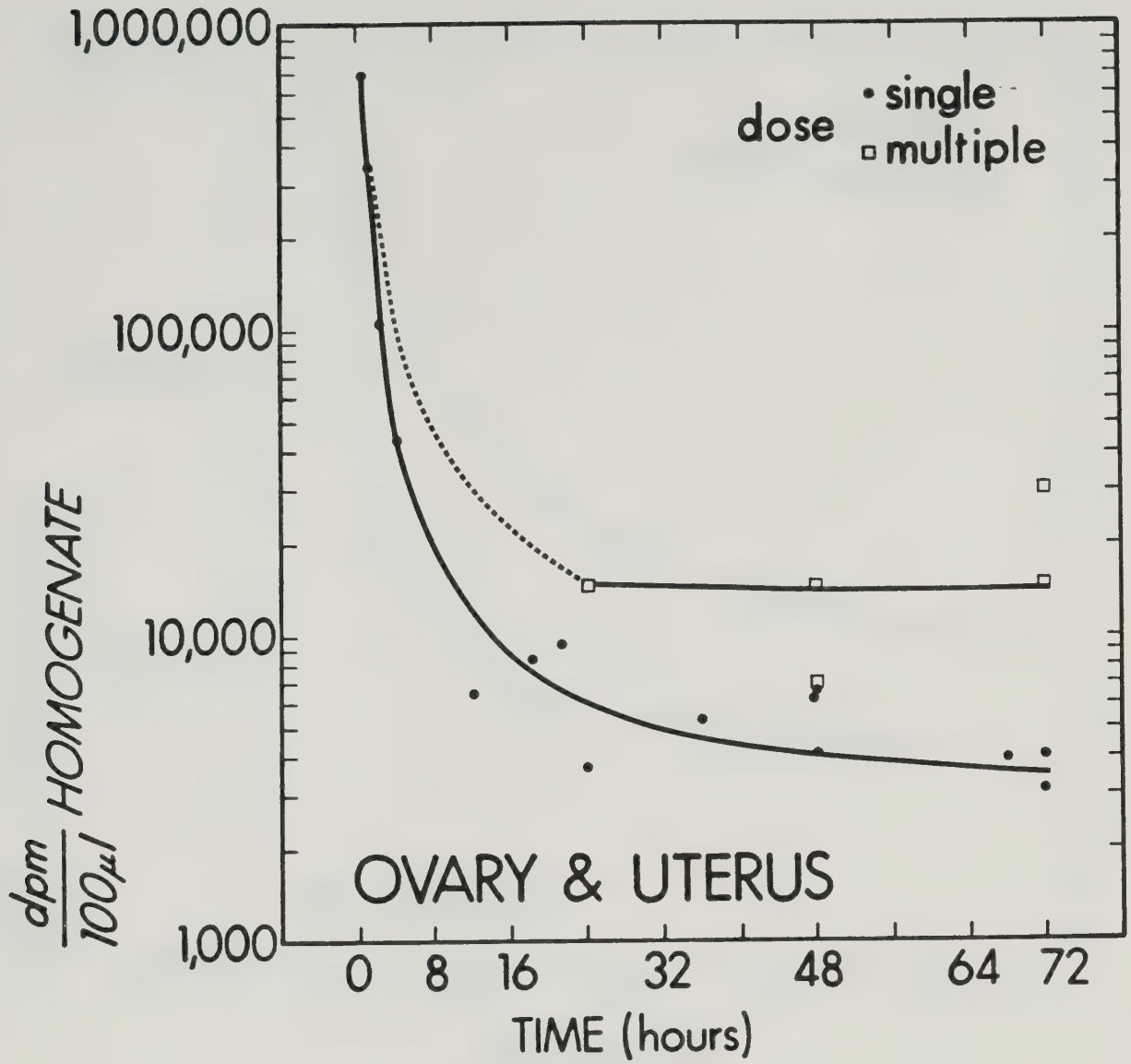

Fig. 13. Amount of ^{14}C-MISO in mouse ovary and uterus correlation coefficient: -0.62 Slope -79.47 for final elimination phase (post 18 hrs.)

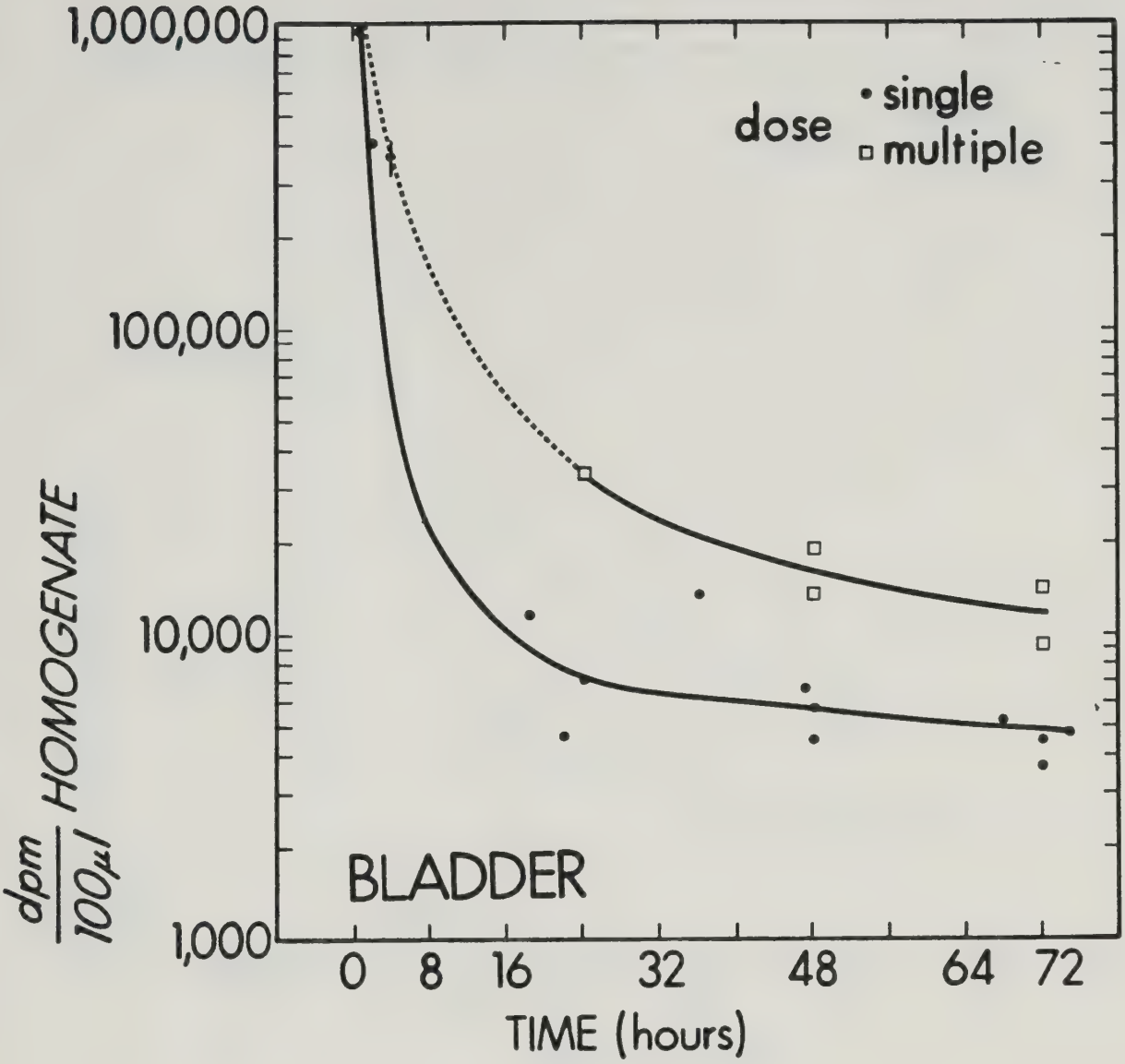

Fig. 14. Amount of ^{14}C-MISO in mouse bladder correlation coefficient: 0.58 Slope -65.67 for final elimination phase (post 18 hrs.)

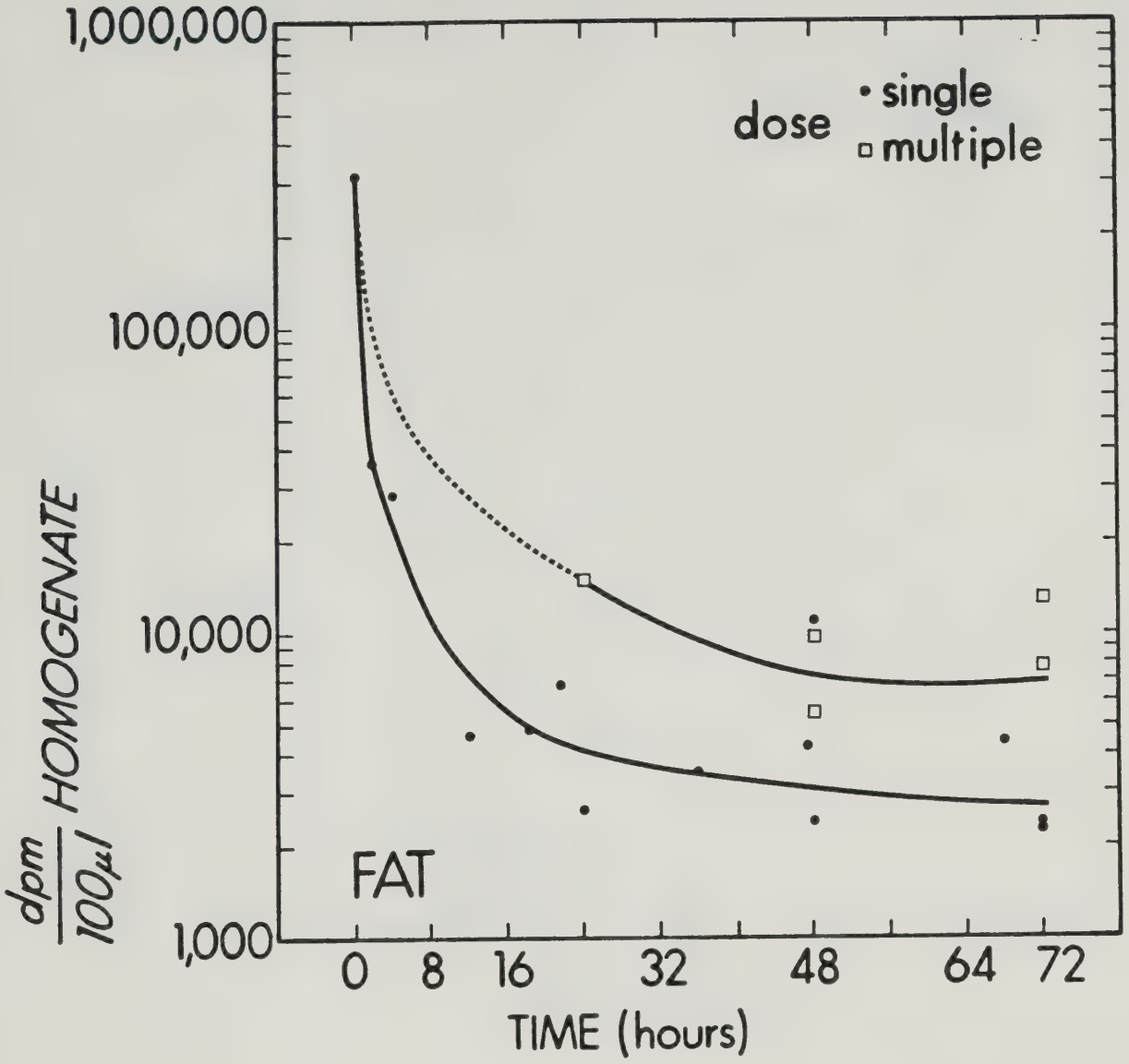

Fig. 15. Amount of ^{14}C-MISO in mouse fat

correlation coefficient: -0.54 Slope -70.0 for final elimination phase (post 18 hrs.)

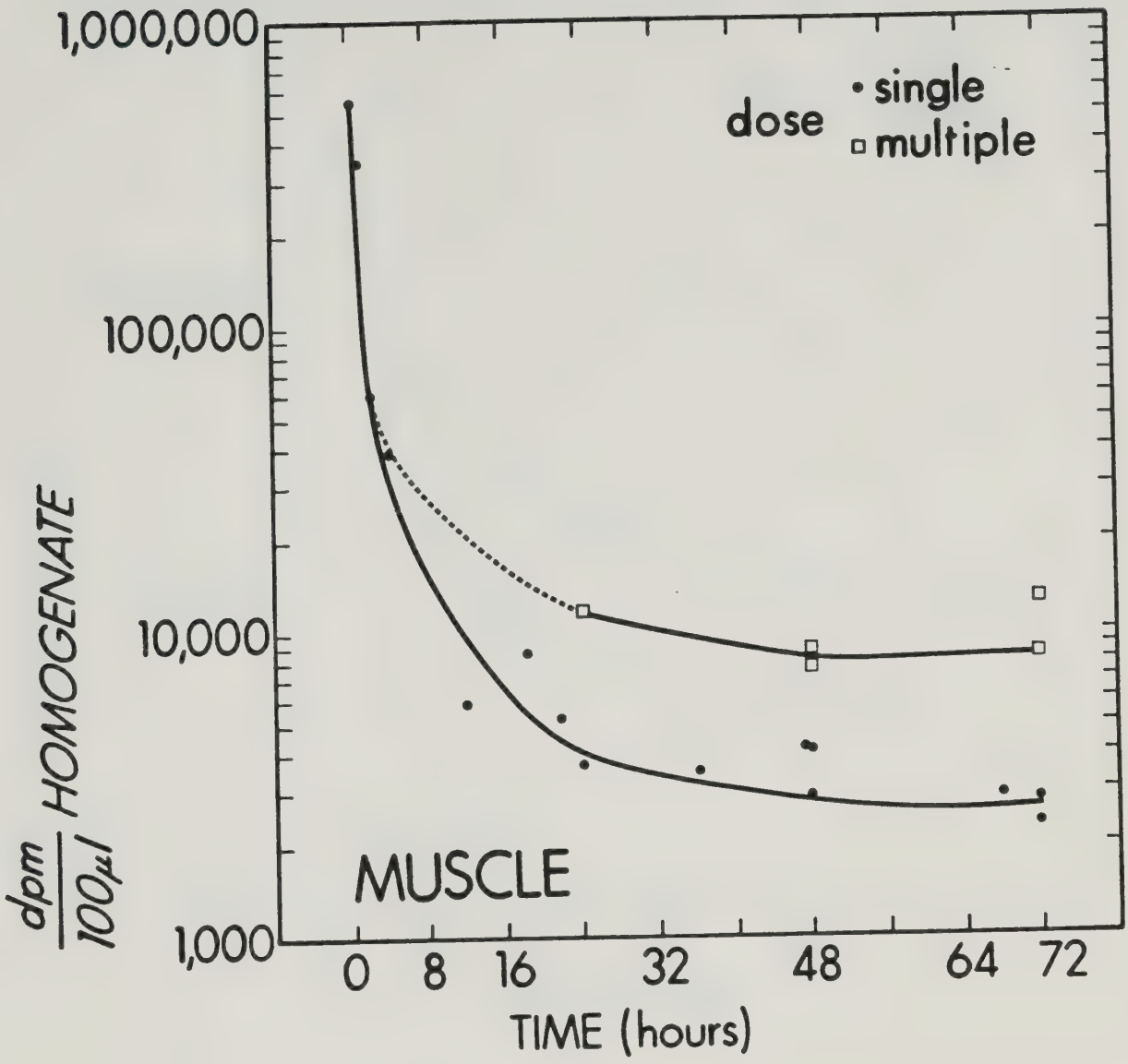

Fig. 16. Amount of ^{14}C-MISO in mouse muscle

correlation coefficient: -0.80 Slope -100.74 for final elimination phase (post 18 hrs.)

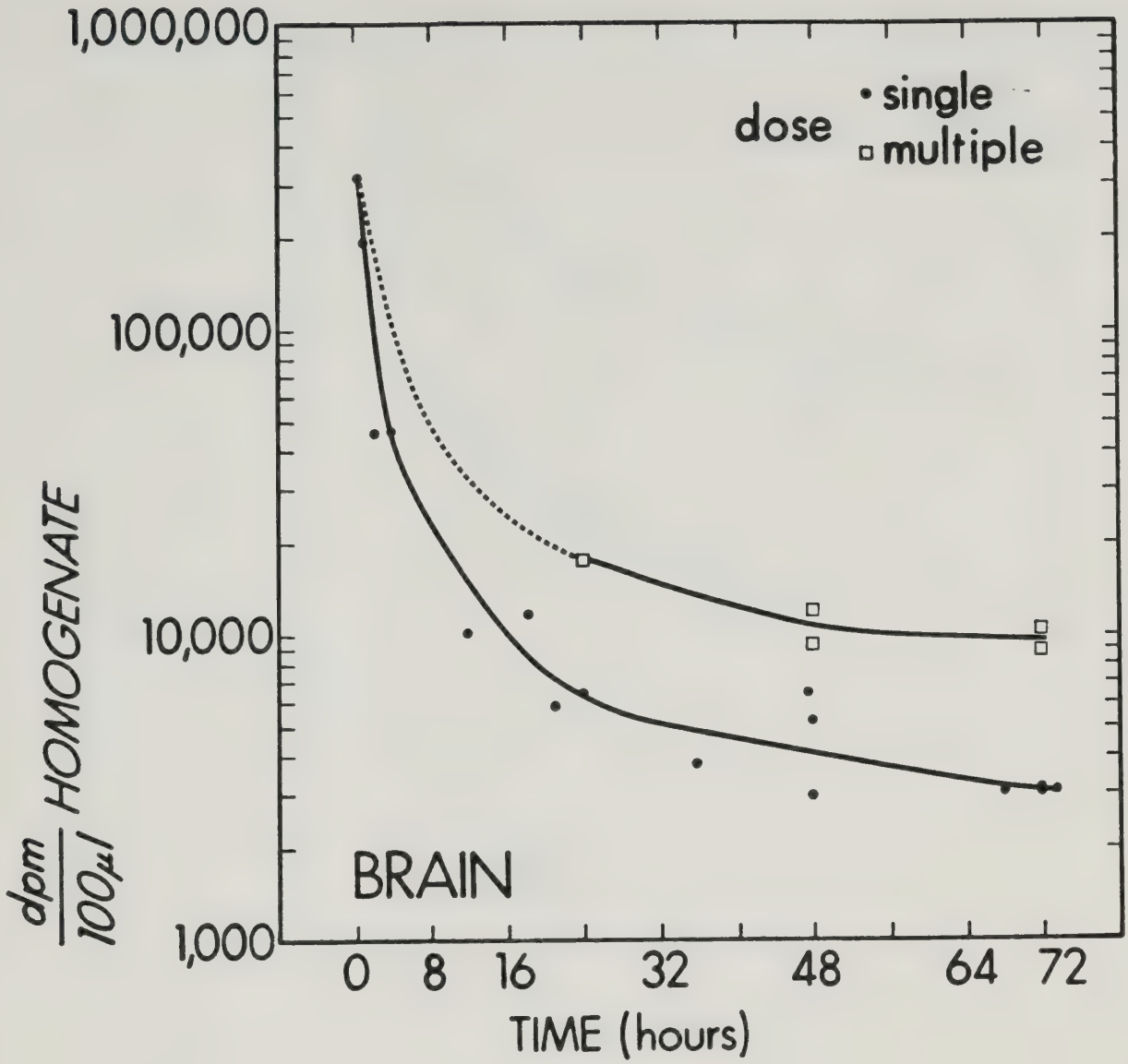

Fig. 17. Amount of ^{14}C-MISO in mouse brain

correlation coefficient: -0.78 Slope -81.85 for final elimination phase (post 18 hrs.)

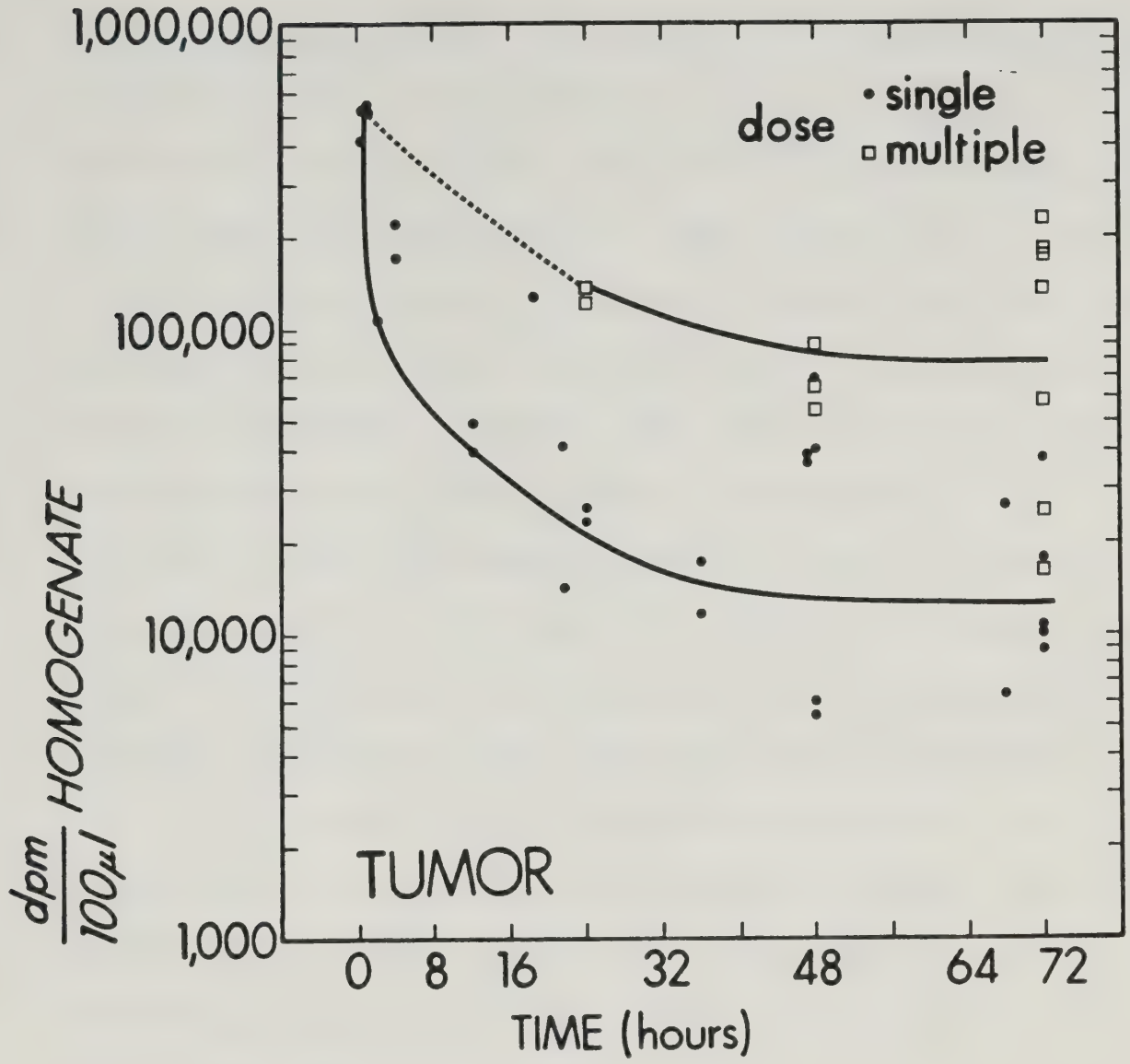

Fig. 18. Amount of ^{14}C-MISO in EMT-6 tumor
correlation coefficient -0.68 Slope -77.3 for
final elimination phase (post 18 hrs.)

including the tumor. At about 12 to 24 hours post injection there was a shift in the slopes of all curves and elimination of the radioactive products appeared to slow down. The half-life of this component of the drug clearance was about 55 hours. Slopes of the latter portion of the curve, (post 18 hours), were fitted by a linear regression program, and corresponding correlation coefficients were also given for each graph.

The absolute amounts of radioactivity within all tissues was at its highest within 30 minutes after injection. Brain and fat had one-half to two-thirds less activity than most other tissues at the 30 minute time.

At all times after the 30 minute sampling time tumor radioactivity levels were substantially higher than blood levels. The blood half-life was calculated to be 36 minutes, slightly different from other reports of 1.0 to 1.5 hours (49).

General trends were for ^{14}C-MISO to clear from all normal tissue except liver to a greater extent than from the tumor. Tissues involved in the elimination of ^{14}C-MISO retained higher concentrations for longer periods of time but eventually stabilized by 24 hours. These tissues are the kidney, bladder and intestine. The liver retained more activity than any other normal tissue.

The clearance of ^{14}C-MISO from tumors followed the same pattern as from normal tissue, but more drug was retained by the tumor. Uptake of ^{14}C-MISO by tumors was highly variable, even among tumors inoculated in the same animal. There was less variability among normal tissues between different animals. Injection of multiple doses of ^{14}C-MISO enhanced uptake in the tumor 2 to 3 times more than in normal tissues. The activity in the tumor compared to the activity in normal tissue is shown in the composite graphs (Fig. 19 & 20). Tumor to tissue ratios (Table I&II) also demonstrate the enhancement. For example, after a single dose the tumor to tissue ratio for the spleen was 4.8; whereas after a multiple dose regimen the ratio was 12.1. This was a 2.5 fold increase. There was increased uptake of ^{14}C-MISO throughout the body, but the retention of radioactivity by the tumor was higher than any other organ, including the liver. Again, there was tremendous variability of ^{14}C-MISO content among tumors.

DISCUSSION

Following a single dose of ^{14}C-MISO there is almost immediate widespread uptake throughout the body (49,50). Tissues with an excellent blood supply would be expected to have the highest concentration of ^{14}C-MISO initially (51), and this is the case with all the tissues sampled

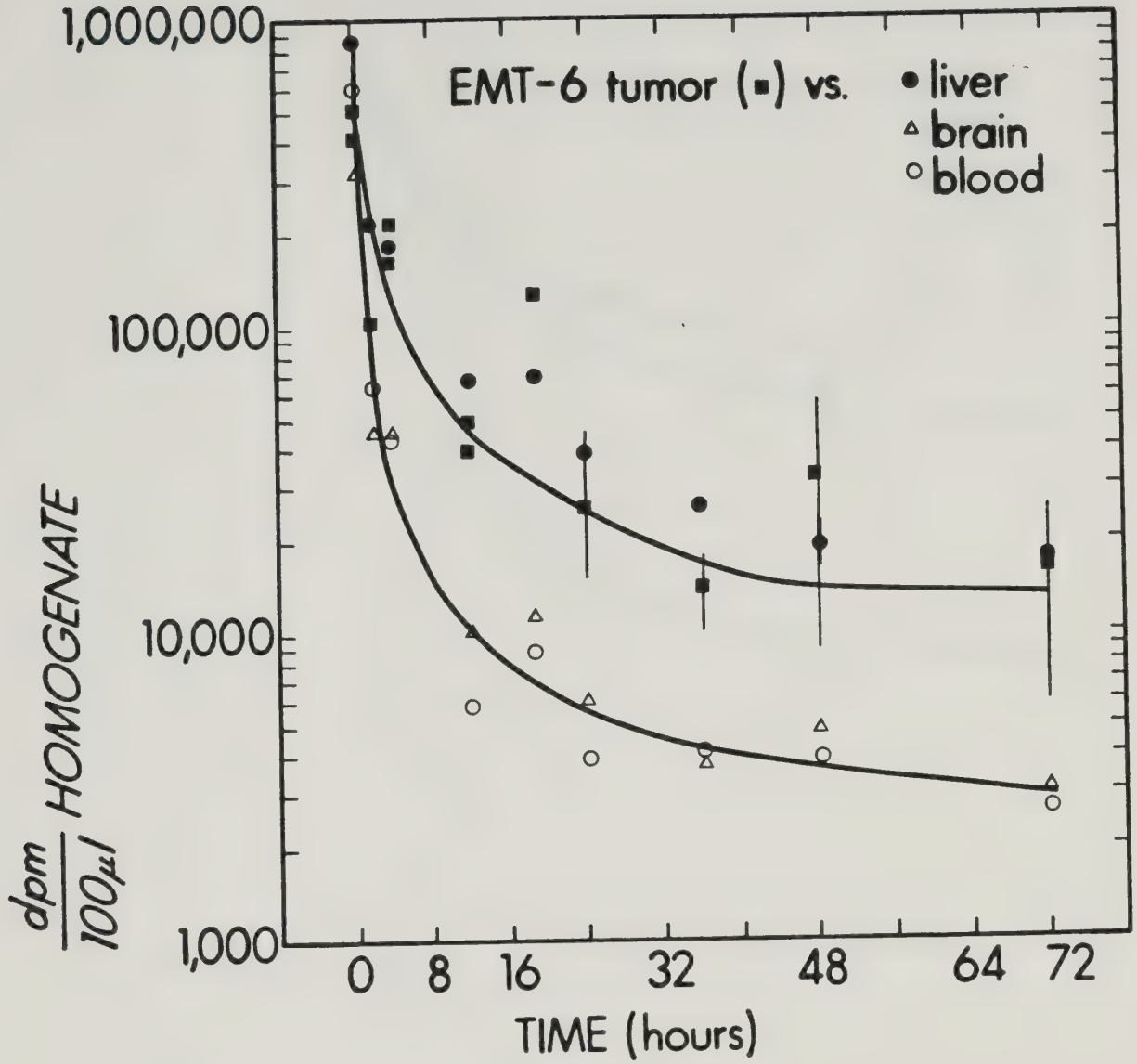

Fig. 19. Composite biodistribution curve for single dose ^{14}C-MISO in BALB/C mice.

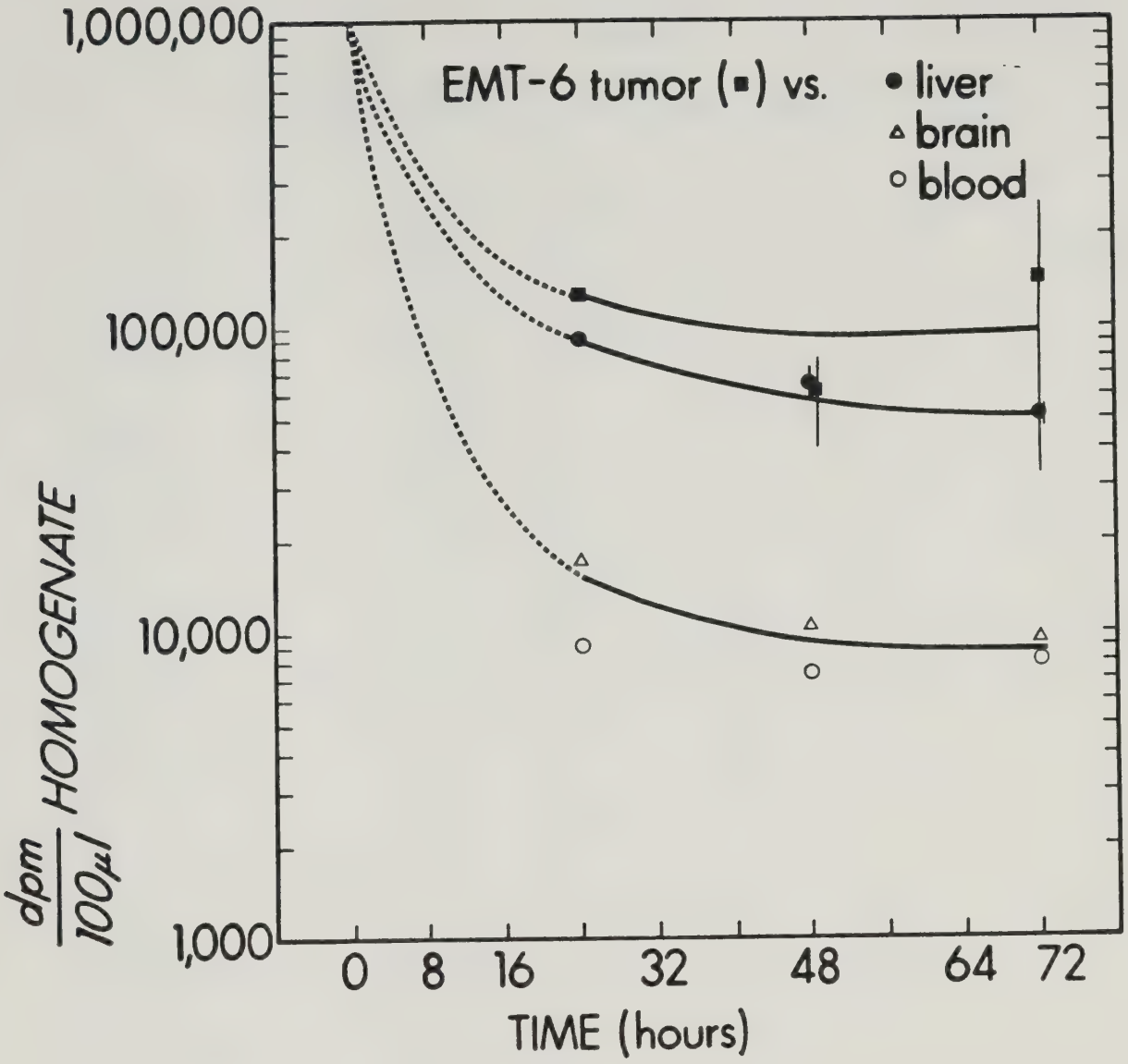

Fig. 20. Composite biodistribution curve for multiple dose ^{14}C-MISO in BALB/C mice.

TABLE I

TUMOR/TISSUE FOR SINGLE DOSE ^{14}C-MISO

TISSUE	24 HR	36 HR	48 HR	72 HR	AVERAGE
Blood	6.5	3.6	2.4	5.6	4.5
Heart	2.5	3.0	1.0	2.4	2.2
Lung	3.1	2.4	1.4	3.4	2.6
Liver	0.7	0.5	0.3	0.8	0.6
Spleen	4.9	3.5	1.9	6.8	4.3
Kidneys	3.2	2.6	1.6	4.1	2.9
Stomach	1.5	1.3	1.3	5.2	2.3
Intestine	3.9	2.1	2.3	8.9	4.3
Colon	3.1	3.8	2.0	5.8	3.7
Ovary & Uterus	6.6	2.8	1.4	4.5	3.8
Bladder	3.4	1.0	1.2	3.8	2.4
Fat	9.1	4.1	2.4	6.6	5.6
Muscle	6.5	4.0	2.0	6.1	4.7
Brain	3.7	3.8	2.0	4.9	3.6

TABLE II

TUMOR/TISSUE FOR MULTIPLE DOSE ^{14}C-MISO

TISSUE	24 HR	48 HR	72 HR	AVERAGE
Blood	14.3	8.1	12.2	11.5
Heart	5.1	2.7	4.4	4.1
Lung	5.9	3.7	6.5	5.4
Liver	1.4	1.0	1.9	1.4
Spleen	11.6	7.5	16.9	12.0
Kidneys	6.7	4.2	6.4	5.8
Stomach	7.2	4.0	9.0	6.7
Intestine	8.9	9.1	26.5	14.8
Colon	5.1	7.8	16.2	9.7
Ovary & Uterus	8.8	6.5	6.7	7.3
Bladder	3.8	3.8	10.7	6.1
Fat	10.0	8.6	12.8	10.0
Muscle	10.9	7.6	8.5	9.0
Brain	7.5	5.9	10.2	7.9

except the brain. Fat, a poorly vascularized tissue, has a low ^{14}C-MISO content. The concentrations of drug within the brain and fat are as much as two-thirds lower than other tissues in the most extreme cases. The low concentration of ^{14}C-MISO within the brain and fat would be expected because of MISO's octanol/water partition coefficient of 0.43 (50). At equilibration a lower concentration of drug would be found in lipid compartments as opposed to water compartments. Both fat and brain have a higher lipid component than other tissues and therefore would be expected to have a lower uptake of MISO.

Liver retains high concentrations of drug (49), almost as high as that in tumors, (after multiple doses of MISO), because it is the body organ responsible for most chemical detoxification pathways (52). Liver microsomes are known to reduce nitroimidazoles such as metronidazole (53) to produce nitro anion radicals. If the radical is exposed to oxygen there is recombination and a return to the original compound. However, in anaerobic conditions the nitro anion radical is further reduced to a toxic intermediate. Autoradiographs of liver exposed to ^{14}C-MISO have shown a homogenous distribution of the drug (54).

Before there is a plateau in radioactivity levels at around 12 to 24 hours, there are occasions when the ^{14}C-MISO content in the gut is higher than in tumors. There could be a number of reasons for this.

(1) Because higher levels only occur up to four hours post injection and disappear after that, there could be some radioactivity remaining at the site of the intraperitoneal injection. This could have been part of the sample when the gut was removed.

(2) The amount of food within the gastrointestinal tract would also affect the amount and clearance of radioactive bile and enzymes secreted by the liver and absorbed by the gut wall.

(3) When the gut was sampled, contents were removed but some residue high in radioactivity may have adhered to the gut wall.

(4) Variability could be due to sampling. Components of the gut could not be removed in their entirety. That is, only segments of the tract were taken, based on their contents. Segments of colon and intestine were removed according to the following criteria: portions of gut containing fluid-like material were intestine and segments of tract holding feces were colon.

(5) Initial high concentrations in the gut may just reflect the normal clearance pathway for MISO (49).

The clearance of ^{14}C-MISO from tumors follows the same pattern as normal tissue, but more activity remains within tumors. Considering tumors as a whole group is difficult because of the tremendous amount of variability in ^{14}C-MISO uptake within this group. This is expected if the labelled drug is a marker for hypoxia. Even within the same animal the uptake and retention of ^{14}C-MISO in the tumors varied by as much as a factor of five. Such differences were found in the same animal in tumors that were inoculated on the same day with the same cell suspension. The fact that the variability was not as great among normal tissues between different animals suggests that MISO behaves differently in a tumor environment than elsewhere in the body. The rate of decline of concentration is probably dependent on the hypoxic fraction present in each tumor. Normal healthy tissues have a good blood supply providing oxygen and nutrients. A tumor will have necrotic and hypoxic cells in addition to healthy proliferating cells. It is highly likely that the MISO binds to the hypoxic cells and remains there, thus lowering the amount of MISO which is free for elimination. Normal tissues do not have this large hypoxic component which would bind the MISO, and MISO is easily washed from the cell. Although concentrations are initially high throughout the body they do not

remain so because unbound MISO is easily excreted. Elimination of this free MISO is probably responsible for the 43 minute half life component of the curve. The amount of MISO retained by normal tissue might be attributed to the smaller hypoxic fraction that probably exists in all tissues. Because of these hypoxic fractions in all tissues, the clearance rates are very similar for all tissues including tumor but the different retained activities are due to bound ^{14}C-MISO. By taking the half-life of each individual tissue and then averaging them all, a half-life of 55 hours is obtained. This is very similar to the half-life of MISO in single cell suspensions of hypoxic EMT-6 cells (55). It is very likely that the half-life in vivo could be attributed to the binding of MISO to hypoxic cells.

The amount of MISO bound to tumors is even more important if it is realized that the MISO may be bound to the hypoxic fraction of the tumor (64). The hypoxic fraction represents only 10 to 30% of the entire tumor. So the tumor to tissue ratios of 2 to 5 for single doses (excluding liver with a ratio of 0.6) could be as much as 10 times higher if one were looking at only the hypoxic zones within the tumor. Multiple dose tumor to tissue ratios of 4 to 15 (excluding liver with a tumor/tissue of 1.4) would also be 3 to 10 times higher if one just looked at the ratio for hypoxic cells only to normal

tissue. Such a concentration in hypoxic tumor tissue would result in acceptable tumor to tissue ratios of greater than 5 for liver and might give a tumor to tissue ratio of up to 150 in some cases. Such signals could be of value in the use of gamma labelled sensitizers as a clinical tool for examining hypoxia within tumors.

The binding of MISO to hypoxic cells can be enhanced by prolonged exposure to the drug. This was demonstrated with *in vitro* experiments (23). If cells were bathed in medium containing MISO for 3 hours under hypoxic conditions, the amount of binding increased. With tumor MISO concentrations achieving a maximum at 30 minutes (55), and with a subsequent half-life of 40 minutes, 3 hour exposure to constant concentrations was not possible with single dose MISO *in vivo*. To simulate prolonged exposure to the radiosensitizer, an initial 20μg/g body weight was given at time 0, followed by 10μg/g at 45 minutes, 10μg/g at 90 minutes and 10μg/g at 135 minutes. This was adequate to maintain drug levels at concentrations that are sufficient for improved binding of MISO to hypoxic cells.

Maintaining a higher concentration of MISO for a prolonged length of time does increase the amount of MISO retained by the tumor relative to the other normal tissues. There is a 2 to 3 fold increase in the tumor to

tissue ratios after multiple dose administration. This strongly suggests that MISO is bound to the macromolecules of hypoxic cells. Otherwise there would be no improvement in tumor to tissue ratios, but just general increased retention of drug throughout the body. Increased binding is not as dramatic *in vivo* as it is *in vitro* because unlike tissue culture the tumors were not 100% hypoxic, and neither is normal tissue 100% oxygenated. A 2 to 3 fold increase in binding to the tumor is exactly what would be expected if a constant concentration of MISO is simulated by the multiple injection procedure. (See Fig. 1). (23). The half-life of MISO in humans is approximately 10 hours (56) and this should produce a greater extent of selective binding to hypoxic cells.

From the data presented in this chapter it can be concluded that MISO does have an affinity for tumors, specifically for the hypoxic cells in the tumor. After clearance, the MISO remains in tumors to a greater extent than in any other tissue. The only exception is the liver and this changes when multiple doses are given. The elimination of MISO follows two patterns: an early rapid phase with a half-life of approximately 43 minutes, and a slower elimination with half-life of 55 hours. The rapid phase is probably due to clearance of free MISO and

desmethyl-MISO, whereas the slow phase is due to removal of bound metabolites. After administration of multiple doses the tumor retains more MISO than any normal tissue including the liver. Tumor to tissue ratios are improved by a factor of 2 to 3 just by giving multiple doses of the drug. This implicates hypoxic cells as being responsible for the increase, based on previous in vitro experiments (23). If the tumor to tissue ratios for hypoxic tumor cells were computed using a hypoxic fraction of 10 to 30% as determined radiobiologically, tumor to tissue ratios of 30 to over 100 result. This makes the proposed clinical use of radiosensitizers labelled with gamma emitting nuclides even more promising.

CHAPTER THREE

UPTAKE OF ^{14}C-MISONIDAZOLE INTO THE HEARTS OF BALB/C MICE TREATED WITH ISOPROTERENOL

INTRODUCTION

Myocardial ischemia can be induced by various methods (57). Coronary vessel ligation is one way, but another method is the injection of drugs. DL-isoproterenol (1[3",4'-dihydroxyphenyl]2-isopropylaminoethanol HCl) dissolved in saline can be injected intraperitoneally to induce cardiac necrosis (58,59). The lesion is uniform in severity and resembles the human myocardial infarction as well as the experimental infarct produced by coronary artery ligation. Isoproterenol can induce infarcts in mice (59), hamster (60), rats and dogs (61) and turtles (62). It has also induced myocardial damage in patients who had received large doses of isoproterenol (63), although this is a rare occurrence. In rats the optimal infarct-producing dose is between 5.25 and 85 mg/kg subcutaneously on 2 consecutive days (57). Mice were shown to have focal degenerative changes in their hearts after one 50 mg/kg subcutaneous dose of isoproterenol (59).

If it can be shown that ischemia or hypoxia can be induced in normal tissue then it could be shown that MISO has an affinity for hypoxic cells, whether they occur in normal tissue or tumor tissue.

RESULTS

Upon death by cervical dislocation the mouse heart was removed and cut in half. Half of the heart was used in liquid scintillation counting and the other half was used for autoradiographs. Liquid scintillation counting of BALB/C mouse heart samples has shown a substantial (approximately 2 fold) increase in the uptake of MISO after treatment with isoproterenol compared with animals treated with saline. (See Fig. 21 and 22). There was an average ratio of 1.6 for those hearts treated with 75μg/g isoproterenol per day for two days prior to ^{14}C-MISO administration and an average ratio of 2.0 for the 200μg/g isoproterenol per day for 2 days. This suggests that as more ischemic damage is induced in the hearts of mice there is more ^{14}C-MISO bound to heart tissue, indicative of hypoxic cells.

DISCUSSION

Associated with the zone of infarction in the heart is an area of ischemic or hypoxic cells and it is hoped that the MISO would have an affinity for these cells as it appears to in the tumor. The studies described in this thesis show that there is 2 fold increase in MISO uptake in the hearts of mice treated with isoproterenol over those with just saline. Increased uptake of ^{14}C-MISO into

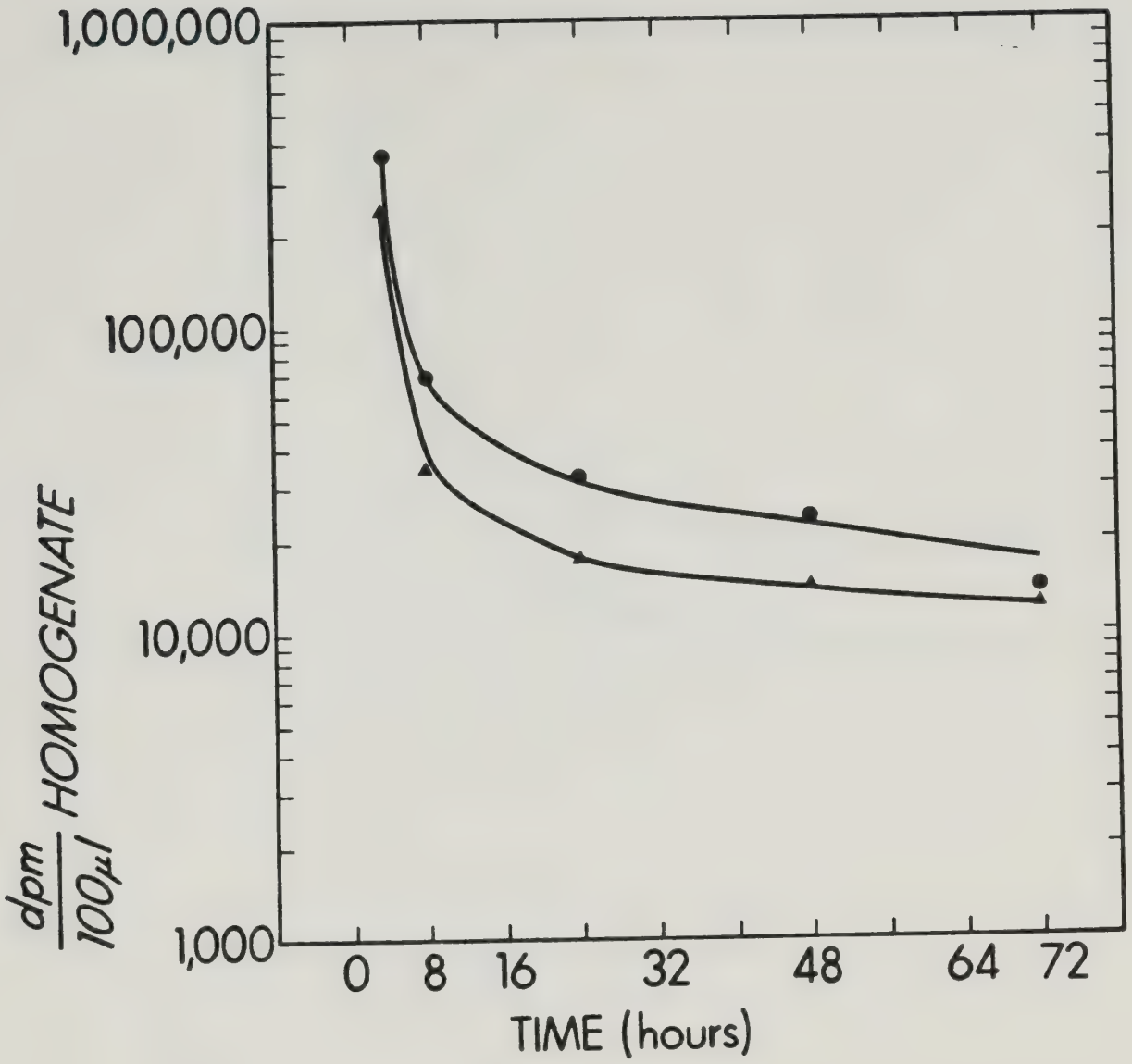

Fig. 21. ^{14}C-MISO uptake into the hearts of BALB/C mice treated with 75µg/g isoproterenol (●) compared to controls (▲).

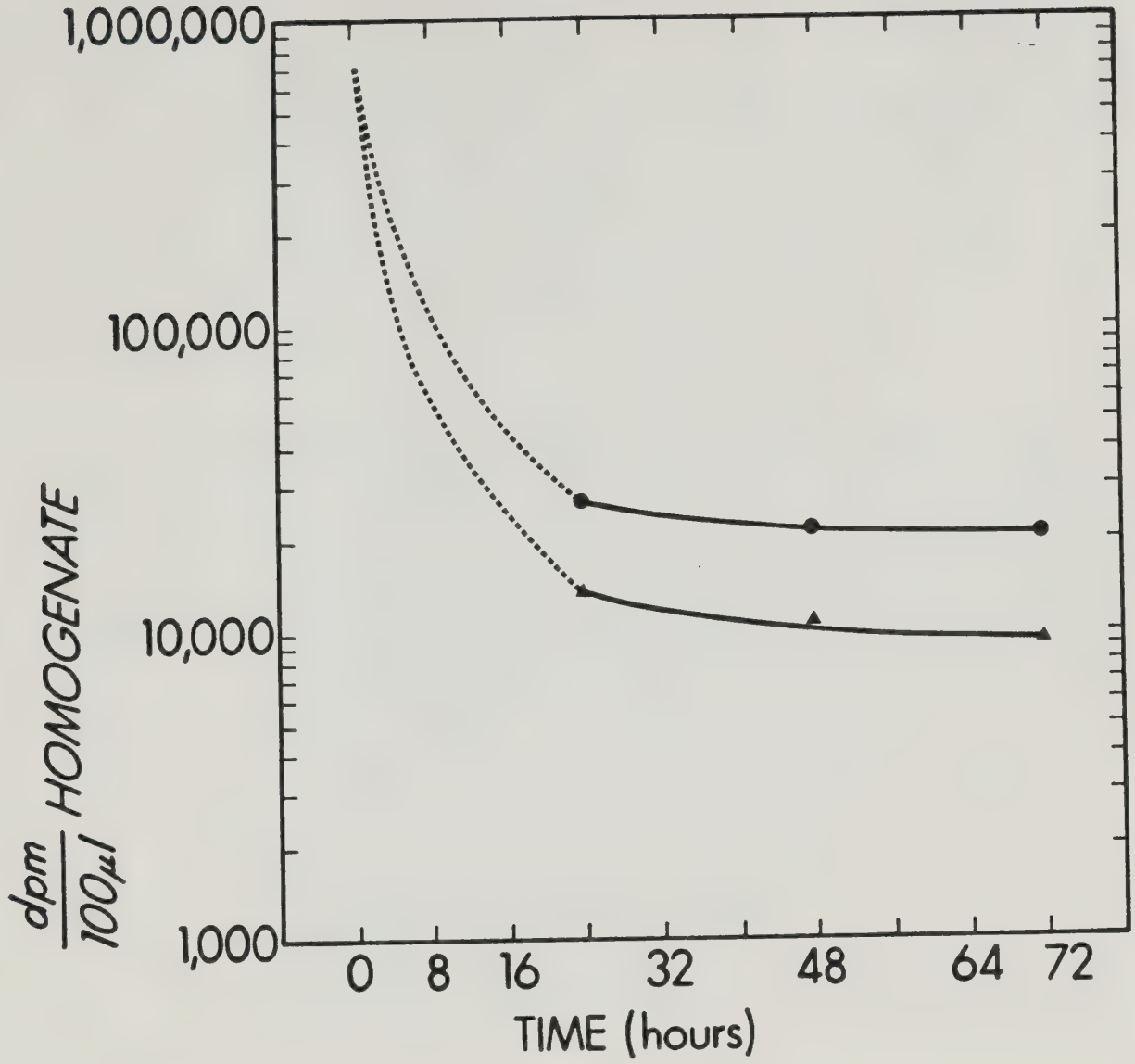

Fig. 22. ^{14}C-MISO uptake into the hearts of BALB/C mice treated with 200µg/g isoproterenol (●) compared to controls (▲).

heart tissue was associated with increased doses of isoproterenol or increased ischemia. This is consistent with the fact that there is a close correlation between the amount of isoproterenol given and the severity of necrosis that occurs in the heart (58). A larger necrotic area would be more likely to have a bigger hypoxic or ischemic zone for which the MISO would have an affinity.

Histological examination of the hearts showed that myocardial ischemia was present. (See Plates C&D). Attempts to demonstrate ^{14}C-MISO uptake with autoradiography were unsuccessful possibly due to interaction of the stain with the photographic emulsion. The increased uptake of ^{14}C-MISO in the ischemic hearts suggests that MISO does have an affinity for hypoxic cells, whether they are in tumors or ischemic hearts.

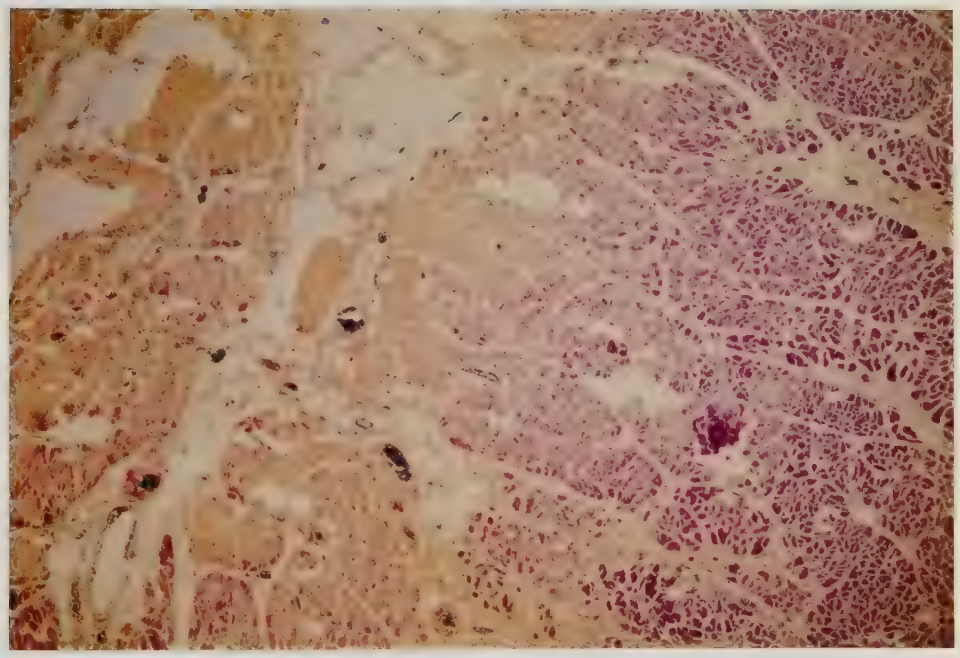

Plate C. Myocardial infarction control specimen demonstrating HBFP stain. Healthy tissue is yellowish brown and infarcted tissue is red.

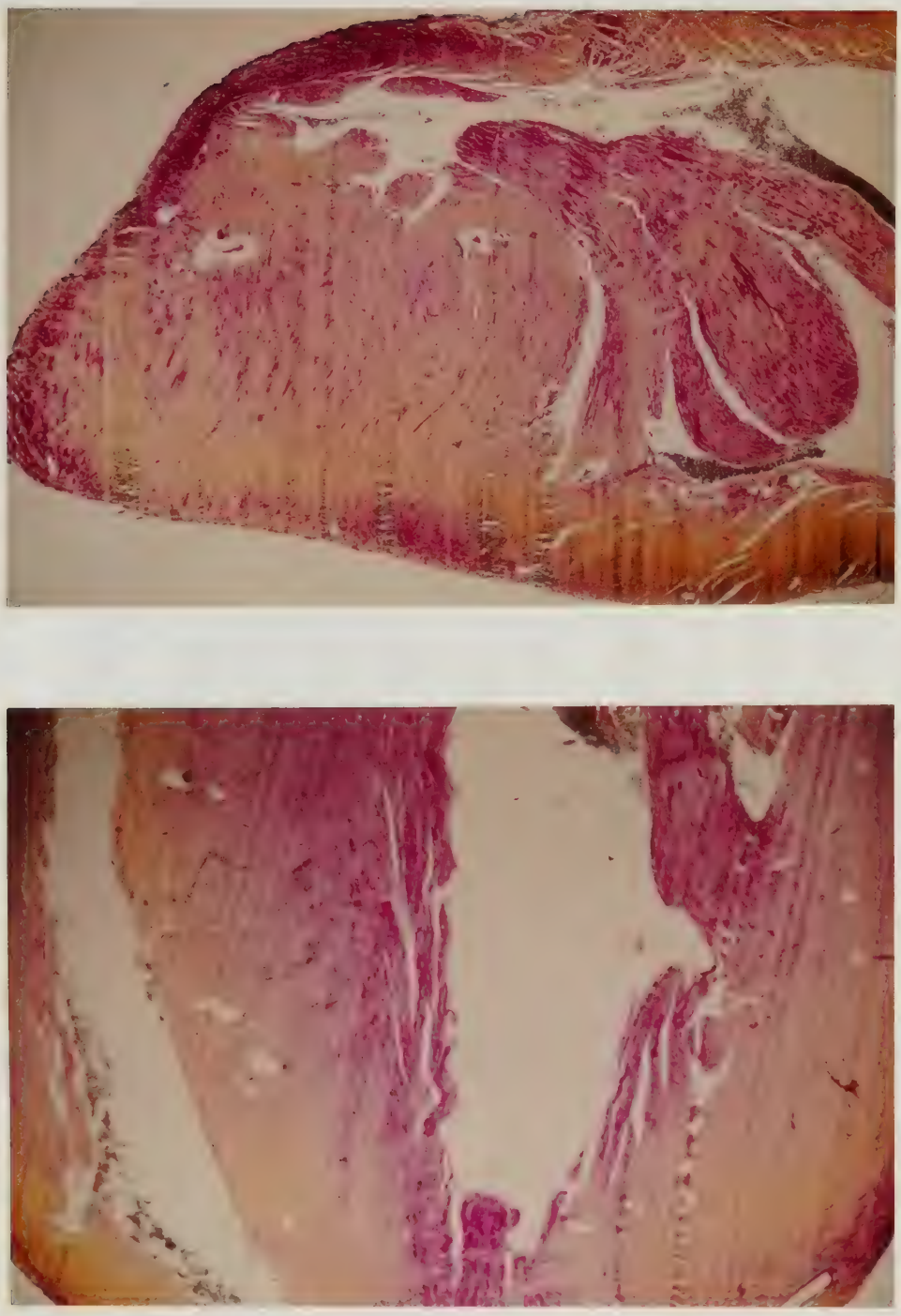

Plate D. Isoproterenol treated heart stained with the HBFP stain. Healthy tissue is yellowish brown and infarcted tissue is red. Attempts to show ^{14}C-MISO uptake with autoradiograph techniques were unsuccessful.

CHAPTER FOUR

WHOLE BODY AUTORADIOGRAPHS SHOWING DISTRIBUTION OF ^{14}C-MISONIDAZOLE IN BALB/C MICE BEARING EMT-6 TUMORS

INTRODUCTION

The technique of whole body autoradiography was first developed by Sven Ullberg to study the distribution of ^{35}S-benzylpenicillin in mice (66). According to Rogers (67), this qualitative method of studying the distribution of drugs has several advantages over the quantitative method of sampling tissues with liquid scintillation counting. When sampling tissues a decision must be made as to which tissues will be examined for their radioactive content. Whole body autoradiography surveys all tissues and organs impartially. Whole body autoradiographs also provide a visual demonstration of the liquid scintillation data which is presented in graphs and tables. It is much easier to see the increased uptake in some organs relative to others simply by looking at one whole body autoradiograph. In the case of the research of this thesis, whole body autoradiographs provide independent confirmation of data obtained using liquid scintillation techniques.

RESULTS

Whole body autoradiographs obtained at Brookhaven National Laboratory, New York, showed high uptake in the tumors and liver. In some cases there was high uptake in the gut and what could be the bladder. Mice were killed 24 hours post single or multiple injection. (See Plates E & F).

Uptake within the tumors was heterogenous. The distribution of radioactivity within the liver and other normal tissue appeared more homogenous.

DISCUSSION

These results provide a qualitative representation of the quantitative data shown in Chapter Two. The high uptake in the liver was expected in view of previous findings. The sections showing high uptake in the gut and bladder indicate the elimination of the ^{14}C-MISO from the body. ^{14}C-MISO appears to have cleared out of all the other organs within 24 hours.

The most important observation is the high uptake in the tumors, which are located along the back of the mouse. Not only is there a high uptake of drug into the tumors but there also appears to be a localization of the drug into areas within the tumor. This suggests that the hypoxic fraction within each tumor is highly variable in degree and pattern. There does not appear to be a

Plate E. Whole body autoradiographs showing ^{14}C-MISO uptake after multiple (upper section) and single (lower section) doses of drug. Tumors, along back of mouse, and liver show high uptake of ^{14}C-MISO.

Plate F. Whole body autoradiograph showing ^{14}C-MISO uptake after multiple doses of drug. The white areas indicate high uptake of radioactivity. High uptake in the lower left portion of the mouse may be in the bladder.

homogenous distribution of MISO within the tumors as there is in the liver. This suggests that although there may be a hypoxic fraction in normal tissues, it is not of the same nature as the hypoxic fraction found in tumors.

These autoradiographs visually demonstrate the liquid scintillation biodistribution data and further encourage the use of a gamma-labelled radiosensitizer as a probe for hypoxia in tumors.

GENERAL DISCUSSION AND CONCLUSIONS

Experiments described in this thesis have demonstrated that the amount of radiolabelled MISO retained by tumors after a single dose is substantially higher than by any other tissue, except the liver. The amount of MISO retained by the tumor after multiple doses is higher than any other tissue including the liver. If only the hypoxic cells within the tumor are considered, the tumor to tissue ratios are even more dramatic; at least 3 to 10 times higher.

MISO clearance follows two phases: a rapid phase (43 min half life) showing the release of free MISO and its major metabolite desmethyl MISO, and a slower phase (55 hr half life) indicating the elimination of the bound adduct in hypoxic cells, whether they exist in healthy tissue or tumors. The residual amount of ^{14}C-MISO in tumor and normal tissues is likely to be bound MISO whose half-life is similar to the half-life of MISO adducts in mammalian cells *in vitro*. It is suggested that the hypoxic cells in the tumor are responsible for the increased retention of the MISO. This is substantiated by the multiple dose data which show increased binding of MISO to mammalian cells with increased exposure time, and by the isoproterenol results which show that MISO does have an affinity for damaged hearts with zones of

hypoxia. Whole body autoradiographs visually demonstrated MISO's affinity for tumors and possibly the hypoxic cells within.

Such results are further encouragement to the use of radiosensitizers labelled with gamma emitting nuclides for noninvasive investigations of hypoxia either within a tumor or in the myocardium as the result of myocardial infarction. By determining the extent of hypoxia in a tumor the radiation therapy regimen could be adjusted accordingly. If a large portion of the tumor contained hypoxic cells, measures to overcome their radioresistance could be taken. Such methods include using hyperbaric oxygen, pretherapy transfusions, fractionated radiotherapy and chemical radiosensitizers such as MISO. As treatment progressed, the extent of hypoxia could also be monitored. Such an investigative tool would be of significant value in tumor treatment planning.

BIBLIOGRAPHY

1. Chapman, J.D. Hypoxic sensitizers - implications for radiation therapy. New England Journal of Medicine 301: 1429-1432 (December 27), 1979.
2. Thomlinson, R.H. and Gray, L.H. The histological structure of some human lung cancers and the possible implications for radiotherapy. British Journal of Cancer 9: 539-549, 1955.
3. Gray, L.H., Conger, A.D., Ebert, M., Hornsey, S. and Scott, O.C.A. The concentration of oxygen dissolved in tissues at the time of irradiation as a factor in radiotherapy. British Journal of Radiology 26: 638-648, 1953.
4. Henk, J.M., Kunkler, P.B., Shah, N.K., Smith, C.W., Sutherland, W.H. and Wassif, S.B. Hyperbaric oxygen in radiotherapy of head and neck carcinoma. Interim report of a controlled clinical trial. Clinical Radiology 21: 223-231, 1970.
5. van den Brenk, H.A.S. Hyperbaric oxygen in radiation therapy. An investigation of dose-effect relationships in tumor response and tissue damage. American Journal of Roentgenology 102: 8-26, 1968.
6. Henk, J.M. and Smith, C.W. Radiotherapy and hyperbaric oxygen in head and neck cancer. Interim report of second clinical trial. The Lancet 2: 104-105, 1977.

7. Henk, J.M. and Smith, C.W. Unequivocal clinical evidence for the oxygen effect. British Journal of Radiology 46: 146, 1973.

8. Bush, R.S., Jenkin, R.D.T., Allt, W.E.C., Beale, F.A., Bean, H., Dembo, A.J. and Pringle, J.F. Definitive evidence for hypoxic cells influencing cure in cancer therapy. British Journal of Cancer 37, Suppl. 3: 302-306, 1978.

9. Urtasun, R.C., Chapman, J.D., Band, P., Rabin, H.R., Fryer, C.G. and Sturmwind, J. Phase I study of high dose metronidazole: a specific in vivo and in vitro radiosensitizer of hypoxic cells. Therapeutic Radiology 117: 129-133, 1975.

10. Awwad, H.K., El Merzabani, M.M., El Badawy, S., Ezzat, S., Akoush, H., Abd El Moneim, H., Saiid, A., Soliman, O., Khafagy, M. and Burgers, M.V. Misonidazole in the preoperative and radical radiotherapy of bladder cancer. Cancer Clinical Trials 3: 275-280, 1980.

11. Bleehen, N.M. The Cambridge glioma trial of misonidazole and radiation therapy with associated pharmacokinetic studies. Cancer Clinical Trials 3: 267-273, 1980.

12. Dische, S. Misonidazole in the clinic at Mount Vernon. Cancer Clinical Trials 3: 175-178, 1980.

13. Dische, S., Gray, A.J. and Zanelli, G.D. Clinical testing of the radiosensitizer RO-07-0582. II. Radiosensitization of normal and hypoxic skin. Clinical Radiology 27: 159-166, 1976.

14. Dische, S., Saunders, M.I., Lee, M.E., Adams, G.E. and Flockhart, I.R. Clinical testing of the radiosensitizer RO-07-0582: experience with multiple doses. British Journal of Cancer 35: 567-579, 1977.

15. Kogelnik, H.D. Clinical experience with misonidazole. High dose fractions versus daily low doses. Cancer Clinical Trials 3: 179-186, 1980.

16. Phillips, T.L., Wasserman, T.H., Johnson, R.J., Levin, V.A. and van Raalte, G. Final report on the United States Phase I clinical trial of the hypoxic cell radiosensitizer, misonidazole (RO-07-0582; NSC #261037). Cancer 48: 1697-1704, 1981.

17. Thomas, G.M., Rauth, A.M., Bush, R.S., Black, B.E. and Cummings, B.J. A toxicity study of daily dose metronidazole with pelvic irradiation. Cancer Clinical Trials 3: 223-230, 1980.

18. Wiltshire, C.R., Workman, P., Watson, J.V. and Bleehen, N.M. Clinical studies with misonidazole. British Journal of Cancer 37, Suppl. 3: 286-289, 1978.

19. Phillips, T.L., Wasserman, T.H., Stetz, J. and Brady, L.W. Clinical trials of hypoxic cell sensitizers. International Journal of Radiation Oncology, Biology, Physics 8: 327-334, 1982.

20. Dische, S., Saunders, M.I., Anderson, P., Stratford, M.R.L. and Minchinton, A. Clinical experience with nitroimidazoles as radiosensitizers. International Journal of Radiation Oncology, Biology, Physics 8: 335-338, 1982.

21. Sealy, R., Williams, A., Cridland, S., Stratford, M., Minchinton, A. and Hallet, C. A report on misonidazole in a randomized trial in locally advanced head and neck cancer. International Journal of Radiation Oncology, Biology, Physics 8: 339-342, 1982.

22. Kapp, D.S., Wagner, F.C. and Lawrence R. Glioblastoma multiforme: treatment by large dose fraction irradiation and metronidazole. International Journal of Radiation Oncology, Biology, Physics 8: 351-355, 1982.

23. Miller, G.G., Ngan-Lee, J. and Chapman, J.D. Intracellular localization of radioactively labelled misonidazole in EMT-6 tumor cells in vitro. International Journal of Radiation Oncology, Biology, Physics 8: 741-744, 1982.

24. Burke, T.R., Johnson, R.J.R., Sako, K., Karakousis, C. and Wojtas, F.D. Development of a durable oxygen microelectrode suitable for implantation to investigate post-surgical tissue hypoxia. Radiation Research 8: 377, 1980.

25. Bicher, H.I., Sandhu, T.S. and Hetzel, F.W. Inhomogeneities in oxygen and pH distributions in tumors. Radiation Research 8: 376, 1980.

26. McNally, N.J. The effect of an hypoxic cell sensitizer on tumour growth delay and cell survival. Implications for cell survival in situ and in vitro. British Journal of Cancer 32: 610-618, 1975.

27. Petterson, E.O. Toxic and radiosensitizing effect of the 2-nitroimidazole misonidazole (RO-07-0582) on murine CFU in vivo. British Journal of Cancer 37, Suppl. 3: 107-110, 1978.

28. Pedersen, J.E., Barron, G. and Meeker, B.E. The value of combining the radiosensitizer misonidazole with cyclophosphamide in treating the murine Lewis lung tumor. International Journal of Radiation Oncology, Biology, Physics 8: 651-653, 1982.

29. Fu, K.K., Hurst, S., Begg, A.C. and Brown, J.M. The effects of misonidazole during continuous low dose rate irradiation. Cancer Clinical Trials 3: 257-265, 1980.

30. Chapman, J.D., Franko, A.J. and Sharplin J. A marker for hypoxic cells in tumours with potential clinical applicability. British Journal of Cancer 43: 546-550, 1981.

31. Tannock, I.F. The relation between cell proliferation and the vascular system in a transplanted mouse mammary tumour. British Journal of Cancer 22: 258-273, 1968.

32. Tannock, I.F. A comparison of cell proliferation parameters in solid and ascites Ehrlich tumors. Cancer Research 29: 1527-1534, 1969.

33. Chapman, J.D., Raleigh, J.A., Pedersen, J.E., Ngan, J., Shum, F.Y., Meeker, B.E. and Urtasun, R.C. Potentially three distinct roles for hypoxic cell sensitizers in the clinic. Radiation Research. Proceedings of the Sixth International Congress of Radiation Research. May 13-19, 1979. Tokyo. Edited by: Okada, S., Imamura, M., Terashima, T. and Yamaguchi, H.. 1979. Japanese Association for Radiation Research, Tokyo, Japan. p. 885-892

34. Fowler, J.F. and Denekamp, J. A review of hypoxic cell radiosensitization in experimental tumors. Pharmaceutical Therapeutics: 413-444, 1979.

35. Lederer, C.M., and Shirley, V.S. (editors). Table of Isotopes. Seventh Edition. John Wiley & Sons, Inc. New York, 1978.

36. Rockwell, S. and Kallman, R.F. Cellular radiosensitivity and tumor radiation response in the EMT6 tumor cell system. Radiation Research 53: 281-294, 1973.

37. Lie, J.T., Holley, K.E., Kampa, W.R. and Titus, J.L. New histochemical method for morphologic diagnosis of early states of myocardial ischemia. Mayo Clinic Proceedings 46: 319-327, 1971.

38. Kallmann, H. and Furst, M. Fluorescence of solutions bombarded with high energy radiation. (Energy transport in liquids). Physical Review 79: 857-870, 1950.

39. Long, E.C. Liquid Scintillation Counting Theory and Techniques. 915-NUC-76-7T Beckman, Beckman Instruments, Inc., Irvine, California, 1976.

40. Baillie, L.A. Determination of liquid scintillation counting efficiency by pulse height shift. International Journal of Applied Radiation and Isotopes. 8: 1-7, 1960.

41. Kerr, V.N., Hayes, F.N. and Ott, D.G. Liquid Scintillation - III. The quenching of liquid-scintillator solutions by organic compounds. International Journal of Applied Radiation and Isotopes 1: 284-288, 1957.

42. Neame, K.D. and Homewood, C.A. Introduction to Liquid Scintillation Counting. The Butterworth Group, London, England. Butterworth & Co. (Publishers) Ltd., London, England, 1974.

43. Rapkin, E. and Gibbs, J.A. Polyethylene containers for liquid scintillation spectrometry. International Journal Applied Radiation Isotopes 14: 71-74, 1963.

44. Price, L.W. Part II, Preparing of samples - I. Lab. Practice 22: 110, 1973.

45. Peng, C.T. Quenching of fluorescence in liquid scintillation counting of labelled organic compounds. Analytical Chemistry 32: 1292-1296, 1960.

46. Dyer,A. An Introduction to Liquid Scintillation Counting. Heyden & Son Ltd., London, 1974.

47. Bush, E.T. General applicability of the channels ratio method of measuring liquid scintillation counting efficiencies. Analytical Chemistry 35: 1024-1029, 1963.

48. Bruno, G.A. and Christian, J.E. Correction for quenching associated with liquid scintillation counting. Analytical Chemistry 33: 650-651, 1961.

49. Chin, J.B. and Rauth, A.M. The metabolism and pharmacokinetics of the hypoxic cell radiosensitizer and cytotoxic agent, misonidazole in C3H mice. Radiation Research 86: 341-357, 1981.

50. Workman, P. Pharmacokinetics of hypoxic cell radiosensitizers. A review. Cancer Clinical Trials 3: 237-251, 1980.

51. Creasey, W.A. Drug Disposition in Humans. The Basis of Clinical Pharmacology. Oxford University Press, New York, 1979.

52. Anthony, C.P. 1967. Textbook of anatomy and physiology. Seventh edition. The C.V. Mosby Company, Saint Louis, p. 389-390.

53. Perez-Rayes, E., Kalyanaraman, B. and Mason, R.P. The reductive metabolism of metronidazole and metronidazole by aerobic liver microsomes. Molecular Pharmacology 17: 239-244, 1980.

54. Chapman, J.D., Baer, K. and Lee, J. Characteristics of the metabolism-induced binding of misonidazole to hypoxic mammalian cells. Cancer Research (in press) 1982.

55. Brown, J.M. Selective radiosensitization of the hypoxic cells of mouse tumors with the nitroimidazoles metronidazole and RO-07-0582. Radiation Research 64: 633-647, 1975.

56. Fowler, J.F., Adams, G.E. and Denekamp, J. Radiosensitizers of hypoxic cells in solid tumors. Cancer Treatment Reviews 3: 227-256, 1976.

57. Rona, G. and Kahn, D.S. Experimental studies on the healing of cardiac necrosis. Annals of the New York Academy of Sciences 156, Art 1: 177-188, 1969.

58. Rona, G., Chappel, C.I., Balazs, T. and Gaudry, R. An infarct-like myocardial lesion and other toxic manifestations produced by isoproterenol in the rat. Archives of Pathology 67: 443-455, 1959.

59. Zbinden, G. and Moe, R.A. Pharmacological studies on heart muscle lesions induced by isoproterenol Annals of the New York Academy of Sciences 156 Art 1: 294-308, 1969.

60. Handforth, C.P. Isoproterenol-induced myocardial infarction in animals. Archives of Pathology 73: 161-165, 1962.

61. Kahn, D.S., Rona, G. and Chappel, C.I. Isoproterenol-induced cardiac necrosis. Annals of the New York Academy of Sciences 156: 285-293, 1969.

62. Ostádel, B., Rychteroá, V. and Poupa, O. Isoproterenol-induced acute experimental cardiac necrosis in the turtle (Testudo Horsfieldi) American Heart Journal 76: 645-649, 1968.

63. Lockett, M.F. Dangerous effects of isoprenaline in myocardial failure. The Lancet 2: 104-106, 1965.

64. Denekamp, J. Biological methods for staging radiosensitization. In: Advanced Topics on Radiosensitizers of Hypoxic Cells. Edited by A. Breccia,

C. Rimondi and G.E. Adams, Plenum Press, New York, p. 119-142, 1982.

65. Flockhart, I.R., Malcolm, S.L., Marten, T.R., Parkins, C.S., Ruane, R.J. and Troup, D. Some aspects of the metabolism of misonidazole. British Journal of Cancer 37, Suppl. 3: 264-267, 1978.

66. Ullberg, S. Studies on the distribution and fat of ^{35}S-labelled benzylpenicillin in the body. Acta Radiologica Supplement 118, 1954.

67. Rogers, A.W. Techniques of autoradiography . Third completely revised edition. Elsevier/North-Holland Biomedical Press, Amsterdam, 1979.